



## Research papers

## Comparison of four nonstationary hydrologic design methods for changing environment

Lei Yan <sup>a</sup>, Lihua Xiong <sup>a,\*</sup>, Shenglian Guo <sup>a</sup>, Chong-Yu Xu <sup>a,b</sup>, Jun Xia <sup>a</sup>, Tao Du <sup>c</sup><sup>a</sup> State Key Laboratory of Water Resources and Hydropower Engineering Science, Wuhan University, Wuhan 430072, China<sup>b</sup> Department of Geosciences, University of Oslo, P.O. Box 1022 Blindern, N-0315 Oslo, Norway<sup>c</sup> Bureau of Hydrology, Changjiang Water Resources Commission, Wuhan 430010, China

## ARTICLE INFO

## Article history:

Received 2 November 2016

Received in revised form 21 April 2017

Accepted 1 June 2017

Available online 3 June 2017

This manuscript was handled by Corrado Corradini, Editor-in-Chief, with the assistance of Ming Ye, Associate Editor

## Keywords:

Nonstationary hydrologic design

Nonstationary flood frequency analysis

Expected number of exceedances

Design life level

Equivalent reliability

Average design life level

## ABSTRACT

The hydrologic design of nonstationary flood extremes is an emerging field that is essential for water resources management and hydrologic engineering design to cope with changing environment. This paper aims to investigate and compare the capability of four nonstationary hydrologic design strategies, including the expected number of exceedances (ENE), design life level (DLL), equivalent reliability (ER), and average design life level (ADLL), with the last three methods taking into consideration the design life of the project. The confidence intervals of the calculated design floods were also estimated using the nonstationary bootstrap approach. A comparison of these four methods was performed using the annual maximum flood series (AMFS) of the Weihe River basin, Jinghe River basin, and Assumpink Creek basin. The results indicated that ENE, ER and ADLL yielded the same or very similar design values and confidence intervals for both increasing and decreasing trends of AMFS considered. DLL also yields similar design values if the relationship between DLL and ER/ADLL return periods is considered. Both ER and ADLL are recommended for practical use as they have associated design floods with the design life period of projects and yield reasonable design quantiles and confidence intervals. Furthermore, by assuming that the design results using either a stationary or nonstationary hydrologic design strategy should have the same reliability, the ER method enables us to solve the nonstationary hydrologic design problems by adopting the stationary design reliability, thus bridging the gap between stationary and nonstationary design criteria.

© 2017 Elsevier B.V. All rights reserved.

## 1. Introduction

Conventional hydrologic design criteria for hydrologic structures are based on the concepts of return period, risk and reliability. These concepts have been used for solving many basic problems in practical engineering design under stationary conditions. However, these concepts must be reformulated and extended to accommodate the nonstationary conditions. As pointed out by the Scientific Decade 2013–2022 of IAHS, entitled “Panta Rhei-Everything Flows” (Montanari et al., 2013), global climate and hydrologic systems are undergoing substantial changes. Many hydrologic variables around the world already exhibit nonstationary behavior due to the effects of climate change and human activities (Milly et al., 2008, 2015).

Nonstationary hydrologic design is essential for coping with changing environment in the future, thus currently becoming one of the research focuses in hydrology. In the nonstationary hydrologic frequency analysis framework, the observations of an extreme hydrologic variable  $Z$ , denoted by  $z_t (t = 1, \dots, k)$  at time  $t$ , are independent but not identically distributed (i/nid) realizations of the nonstationary distribution  $G_Z(z|\theta_t)$  for the year  $t$  with parameters  $\theta_t$  varying with time (Read and Vogel, 2015; Rootzén and Katz, 2013; Salas and Obeysekera, 2014; Villarini et al., 2009; Katz et al., 2002) or other covariates including precipitation, irrigated area, harvested grain area, reservoir indices and population (Yan et al., 2017; Condon et al., 2015; Du et al., 2015; Jiang et al., 2015b; Mondal and Mujumdar, 2015; López and Francés, 2013; Gilroy and McCuen, 2012; Villarini et al., 2009, 2015; Villarini and Strong, 2014). Accordingly, for a specific design value  $Z_q$ , the annual exceedance probability at year  $t$ , denoted by  $p_t$ , is given by  $p_t = 1 - G_Z(z_q|\theta_t)$ . With respect to the hydrologic design of nonstationary flood events, how to determine the return period of the given design value  $Z_q$  under nonstationary conditions is one

\* Corresponding author.

E-mail addresses: [yanl@whu.edu.cn](mailto:yanl@whu.edu.cn) (L. Yan), [xiongh@whu.edu.cn](mailto:xiongh@whu.edu.cn) (L. Xiong), [siguo@whu.edu.cn](mailto:siguo@whu.edu.cn) (S. Guo), [c.y.xu@geo.uio.no](mailto:c.y.xu@geo.uio.no) (C.-Y. Xu), [xiajun666@whu.edu.cn](mailto:xiajun666@whu.edu.cn) (J. Xia), [dtgege@126.com](mailto:dtgege@126.com) (T. Du).

of the core questions. If we follow the definition of the return period under stationary conditions, it has been suggested that, given the nonstationary probability function, the corresponding annual return period  $m_t$  associated with  $Z_q$  is determined as  $m_t = 1/p_t = 1/(1 - G_z(z_q|\theta_t))$ . Obviously, this kind of definition of the annual return period for the given design value under a changing environment would not be very convincing or convenient for many hydrologic design problems in real-world applications as the value of the return period calculated for a given design value would change from one year to another year (Cooley, 2013; Du et al., 2015; Liang et al., 2016; Read and Vogel, 2016; Salas and Obeysekera, 2014). Thus, the definition of the annual return period for the given design value under changing environment needs to be carefully defined.

Initially, there were two different interpretations of return periods for estimating design floods considering the nonstationarity of flood distributions, without considering the design lifespan of water resources projects. In one interpretation, the return period, denoted by  $m$  (years), is defined as the expected waiting time (EWT) until an exceedance occurs (Olsen et al., 1998; Salas and Obeysekera, 2014), while in the other interpretation, the return period is defined as the time period that results in the expected number of exceedances (ENE) over this time period being equal to one (Parey et al., 2007, 2010). However, as pointed out by Rootzén and Katz (2013), and also by Read and Vogel (2015), the flood return levels calculated by the EWT and ENE methods are not directly associated with the project's design life period. Besides, the EWT method may require infinite exceedance probabilities to guarantee its mathematical convergence (Read and Vogel, 2015; Liang et al., 2016), and the rate of convergence of EWT may be significantly different depending on the selection of distributions. These issues are all challenges facing the practical application of EWT and ENE in future hydrologic design.

Under changing environment, we must associate design floods with the design life period of projects to ensure the hydrologic design is really relevant to the operation of the hydrologic projects, because the design value for a given exceedance probability over the project life period would be significantly different from that over other time periods of the same length due to the nonstationarity of probability distributions. For example, under a changing environment, the design value for a hydrologic structure constructed to be in service during 2015–2064 is certainly different from that for a structure planned to be in service during 2050–2099. Therefore, for nonstationary hydrologic design, the lifespan of a hydrologic structure should be taken into consideration (Rootzén and Katz, 2013; Salas and Obeysekera, 2014; Serinaldi, 2015; Read and Vogel, 2015; Liang et al., 2016).

Several hydrologic design methods that take the design life period of projects into account have been proposed in recent years. The first of such methods is the concept of the "design life level" proposed by Rootzén and Katz (2013), which is used to calculate the design value corresponding to a given reliability during a project's design life period. In this paper, the beginning year of operation for the project in the design is denoted by  $T_1$ , the end year by  $T_2$ , and the project's design life period by  $T_1 - T_2$ . Likewise, Salas and Obeysekera (2014) proposed a definition of system reliability over the design life period  $T_1 - T_2$  of projects, denoted by  $RE_{T_1-T_2}^{ns}$  where  $RE$  represents "reliability" and the superscript  $ns$  represents "nonstationary", and stipulated that the probability that no extreme event would exceed the design value over  $T_1 - T_2$  as  $RE_{T_1-T_2}^{ns}$ . The mathematical expression of the reliability  $RE_{T_1-T_2}^{ns}$  under nonstationary conditions is identical to that of DLL in nature but is different in terms of their starting points and applications. This is because  $RE_{T_1-T_2}^{ns}$  is applied to verify the reliability of an existing project while DLL is used in a design situation to estimate the

design value corresponding to a given reliability. The second such method is the concept of "equivalent reliability" (ER) proposed by Liang et al. (2016), who argued that the reliability during the lifespan of hydrologic structures under nonstationary conditions, i.e.,  $RE_{T_1-T_2}^{ns}$ , should be identical to the reliability under stationary conditions, denoted by  $RE_{T_1-T_2}^s$ .

Read and Vogel (2015) summarized existing theories in hydrologic design under both stationary and nonstationary conditions to provide comprehensive descriptions and discussions of the probabilistic behaviors of the return period and reliability. They also proposed a new measure of system reliability of hydrologic structures over the design life period following Stedinger and Crainiceanu (2000), which is termed as "annual average reliability", denoted by  $RE_{T_1-T_2}^{ave}$ , and is mathematically equal to the average value of annual non-exceedance probabilities over the project's design lifespan. Inspired by the concept of "annual average reliability", this paper proposes the concept of "average design life level" (ADLL) for the hydrologic design under a changing environment. It should be noted that a similar definition in a continuous form has been proposed by Buchanan et al. (2016) for extreme coastal flood heights risk analysis.

To highlight the significance of considering the project's design life period in nonstationary hydrologic design, this paper aims to compare four different nonstationary hydrologic design methods, i.e., the DLL method proposed by Rootzén and Katz (2013), the ENE method presented by Parey et al. (2007, 2010), the ER method introduced by Liang et al. (2016), and the ADLL method based on Read and Vogel (2015), in calculating design floods under a changing environment (with the estimated stationary design floods serving as a benchmark for comparison). To clearly demonstrate the differences in hydrologic design values between different design methods for different nonstationarity scenarios, the applications and comparisons of the four methods for estimating nonstationary design floods and the associated confidence intervals (CIs) are demonstrated by using the annual maximum flood series (AMFS) of three representative basins whose hydrologic processes have been affected by growing population and human intervention, i.e., the Weihe River basin (WRB) and the Jinghe River basin (JRB) in northwestern China and the Assumpink Creek basin (ACB) at Trenton, New Jersey. These three basins are representative since they include both decreasing and increasing trends of AMFS, and also have different underlying surface conditions (large basins with complex terrain and a small highly urbanized basin).

This paper is organized as follows. Section 2 presents the methodologies and theoretical analysis of the four nonstationary hydrologic design methods (ENE, DLL, ER and ADLL), the nonstationary flood frequency analysis method, along with a brief description of nonstationary bootstrap method and approaches used for projecting future covariates, i.e., the statistical downscaling method and logistic growth model. In Section 3, we describe the study areas and the data sets used in this study. The applications and results of different methods are demonstrated in Section 4. Finally, the conclusions along with some discussions are included in Section 5.

## 2. Methodology

In this section, the methodologies and the theoretical analysis of the four methods for estimating design floods under nonstationary conditions are first presented (Section 2.1). Second, the methodology of the nonstationary flood frequency analysis is described (Section 2.2). Third, the statistical downscaling method and logistic growth model used to project local future precipitation and population are briefly introduced (Section 2.3). Finally, the

nonstationary nonparametric bootstrap method for calculating confidence intervals is described (Section 2.4).

### 2.1. Four methods for calculating hydrologic design values under nonstationary conditions

Among the four methods to be compared, both the ENE and ER methods are return period based methods, while DLL and ADLL are risk/reliability based methods which estimate design values for given probability values of risk or reliability. However, the four methods can be unified together under a general framework through a relationship transforming the so-called representative reliability (*RRE*) into the return period, i.e.,  $m = 1/(1 - RRE)$ , in which we compute the return period  $m$  using the representative reliability *RRE*. For each different method, the definition formula of *RRE* will be different, as shown below. The four nonstationary hydrologic design methods are described in the subsequent four sub-sections, i.e., ENE (Section 2.1.1), DLL (Section 2.1.2), ER (Section 2.1.3) and ADLL (Section 2.1.4), followed by the theoretical analysis of the four nonstationary hydrologic design methods (Section 2.1.5).

#### 2.1.1. Expected number of exceedances (ENE)

The ENE method was proposed by Parey et al. (2007, 2010) and then propagated by Cooley (2013). In this method,  $N$  is defined as the number of exceedances of the hydrologic variable  $z_t$  over the design value  $z_q$  in  $m$  years, then  $N = \sum_{t=1}^m I(z_t > z_q)$  under nonstationary conditions, where  $I(\cdot)$  is an indicator variable representing whether the hydrologic variable  $z_t$  is larger than the design value  $z_q$ . Thus, the expected value of  $N$  is defined as

$$E(N) = \sum_{t=1}^m E[I(z_t > z_q)] = \sum_{t=1}^m P(z_t > z_q) = \sum_{t=1}^m (1 - G_Z(z_q | \theta_t)) \quad (1)$$

In the ENE method, the design value with an  $m$ -year return period is denoted by  $z^{ENE}(m)$ , for which the expected number of exceedances in the  $m$ -year period is equal to one. Therefore,  $z^{ENE}(m)$  is the solution to the following equation:

$$1 = \sum_{t=1}^m (1 - G_Z(z^{ENE}(m) | \theta_t)) \quad (2)$$

Under this ENE assumption, the assumed representative reliability of water resources projects under the design value corresponding to the  $m$ -year return period can be derived as  $RRE^{ENE} = \sum_{t=1}^m G_Z(z^{ENE}(m) | \theta_t) / (1 + \sum_{t=1}^m G_Z(z^{ENE}(m) | \theta_t))$ .

By assuming that the frequency of extreme events follows the Poisson binomial distribution, Obeysekera and Salas (2016) also considered a case where the value of ENE could be equal to or greater than one. Another interpretation of the return period under nonstationary conditions is that the expected waiting time (EWT) until an exceedance of the design value occurs is just the return period (Olsen et al., 1998; Salas and Obeysekera, 2014). However, in cases with either increasing or decreasing trends, the EWT method may require knowing exceedance probabilities for an infinite future time period, which is impossible to predict with any certainty, to guarantee its convergence (Cooley, 2013; Du et al., 2015; Read and Vogel, 2015; Liang et al., 2016). In addition, the rate of convergence of EWT may differ significantly depending on which distribution is chosen to fit the extreme events. Due to these application restrictions, the EWT method is not considered for comparison in this paper.

#### 2.1.2. Design life level (DLL)

Rootzén and Katz (2013) proposed the “design life level” concept corresponding to the reliability  $RE_{T_1-T_2}^{ns}$  of water resources projects, which is defined as:

$$RE_{T_1-T_2}^{ns} = \prod_{t=T_1}^{T_2} (1 - p_t) = \prod_{t=T_1}^{T_2} G_Z(z_q | \theta_t) \quad (3)$$

In fact, this definition of reliability  $RE_{T_1-T_2}^{ns}$  is the probability that the concerned extreme hydrologic variable  $Z$ , such as annual maximum flood, is less than the design value  $z_q$  for each of every single year over the design period  $T_1 - T_2$  of projects under nonstationary conditions, just the same as defined by Salas and Obeysekera (2014). So it can also be written as:

$$RE_{T_1-T_2}^{ns} = F_{T_1-T_2}(z_q) = \prod_{t=T_1}^{T_2} G_Z(z_q | \theta_t) \quad (4)$$

This reliability  $RE_{T_1-T_2}^{ns}$  can then be transformed into a return period  $m$  via  $m = 1/(1 - RE_{T_1-T_2}^{ns})$ . Denote the design life level corresponding to the return period  $m$  over the period  $T_1 - T_2$  by  $z_{T_1-T_2}^{DLL}(m)$ , then it can be calculated as

$$z_{T_1-T_2}^{DLL}(m) = F_{T_1-T_2}^{-1}(1 - 1/m) \quad (5)$$

In this case, the assumed representative reliability of water resources projects under the design value corresponding to the  $m$ -year return period is just derived as

$$RRE^{DLL} = F_{T_1-T_2}(z_{T_1-T_2}^{DLL}(m)) = \prod_{t=T_1}^{T_2} G_Z(z_{T_1-T_2}^{DLL}(m) | \theta_t).$$

#### 2.1.3. Equivalent reliability (ER)

Liang et al. (2016) proposed the concept of “equivalent reliability” (ER) to estimate design floods under nonstationary conditions. In this approach, although the design values for a given design period might be different under stationary and nonstationary conditions, the design values calculated using conventional stationary hydrologic design and nonstationary hydrologic design should have the same reliability during the lifespan of projects. Under stationary conditions, if a project is designed to withstand a flood event that occurs once in  $m$  years, then the reliability within the design life period  $T_1 - T_2$  of the project is given by

$$RE_{T_1-T_2}^s = \left(1 - \frac{1}{m}\right)^{T_2-T_1+1} \quad (6)$$

where the superscript  $s$  represents “stationary”. However, under nonstationary conditions, the reliability that no flood exceeds the design value  $z_q$  during the design life period  $T_1 - T_2$  is defined by Eq. (3) (Salas and Obeysekera, 2014).

Assuming that  $RE_{T_1-T_2}^s = RE_{T_1-T_2}^{ns}$ , then the design value for the given return period  $m$  based on the concept of ER is denoted by  $z_{T_1-T_2}^{ER}(m)$ , which is the solution to the following equation:

$$\prod_{t=T_1}^{T_2} G_Z(z_{T_1-T_2}^{ER}(m) | \theta_t) = \left(1 - \frac{1}{m}\right)^{T_2-T_1+1} \quad (7)$$

For the ER method, the assumed representative reliability of water resources projects under the design value associated with the  $m$ -year return period can be derived as

$$RRE^{ER} = \left( \prod_{t=T_1}^{T_2} G_Z(z_{T_1-T_2}^{ER}(m) | \theta_t) \right)^{1/(T_2-T_1+1)}.$$

When using the ER method, with the return period  $m$  and design life period given, we can obtain the value on the right side of Eq. (7) first, and eventually obtain the design value  $z_{T_1-T_2}^{ER}(m)$  corresponding to  $m$  by solving this equation. The ER method enables us to solve design problems under nonstationary conditions by adopting the stationary design reliability, thus possibly avoiding practical application problems arising from the imperfect nonstationary theory and allowing relationships to be established between stationary and nonstationary design strategies.

#### 2.1.4. Average design life level (ADLL)

Based on previous studies (Stedinger and Crainiceanu, 2000), Read and Vogel (2015) introduced another measure of reliability termed the “annual average reliability”, which is defined as

$$RE_{T_1-T_2}^{ave} = \frac{1}{T_2 - T_1 + 1} \sum_{t=T_1}^{T_2} (1 - p_t) = \frac{1}{T_2 - T_1 + 1} \sum_{t=T_1}^{T_2} G_Z(z_q | \theta_t) \quad (8)$$

Following Eq. (8), a new definition of the annual maximum flood probability distribution of the design value  $z_q$  over a project's design life period  $T_1 - T_2$  is presented by

$$H_{T_1-T_2}(z_q) = RE_{T_1-T_2}^{ave} = \frac{1}{T_2 - T_1 + 1} \sum_{t=T_1}^{T_2} G_Z(z_q | \theta_t) \quad (9)$$

where  $H_{T_1-T_2}(z_q)$  in nature is a mixture distribution model with the equal weight of  $1/(T_2 - T_1 + 1)$  assigned to each year's probability distribution  $G_Z(z_q | \theta_t)$  within the project's design life period from  $T_1$  to  $T_2$ . Assuming  $m = 1/(1 - H_{T_1-T_2}(z_q))$ , then the “average design life level” corresponding to return period  $m$  over  $T_1 - T_2$ , denoted by  $z_{T_1-T_2}^{ADLL}(m)$ , is derived from the following equation:

$$\frac{1}{T_2 - T_1 + 1} \sum_{t=T_1}^{T_2} G_Z(z_{T_1-T_2}^{ADLL}(m) | \theta_t) = 1 - 1/m \quad (10)$$

$z_{T_1-T_2}^{ADLL}(m)$  has an average  $1/m$  yearly probability of occurrence over the period  $T_1 - T_2$ . In this method, the assumed representative reliability of water resources projects under the design value of the  $m$ -year return period is given by

$$RRE^{ADLL} = H_{T_1-T_2}(z_{T_1-T_2}^{ADLL}(m)) = \frac{1}{T_2 - T_1 + 1} \sum_{t=T_1}^{T_2} G_Z(z_{T_1-T_2}^{ADLL}(m) | \theta_t).$$

It should be noted that there are two other yearly reliability/risk measures. One is the Average Annual Design Life Level (AADLL), proposed by Buchanan et al. (2016), which is similar to ADLL proposed in this study. The difference is that ADLL is in the discrete form whereas AADLL is in the continuous form. The other measure is the Minimax Design Life Level proposed by Rootzén and Katz (2013), denoted by  $T_1 - T_2 p\%$ , which is called bounded yearly risk level and represents design value that results in the probability of exceedance for each year being at most  $p\%$  over the period  $T_1 - T_2$ .

#### 2.1.5. Theoretical analysis of the four nonstationary hydrologic design methods

The ENE method proposed by Parey et al. (2007, 2010), i.e., Eq. (2), to derive the flood return level for the return period of  $m$  years is merely a special case of Eq. (10). If the initial year of the ENE method is set to be the same as the beginning year  $T_1$  of the structure, according to the ENE method defined by Eq. (2), the  $m$ -year return level  $z^{ENE}(m)$  can be calculated by

$$\sum_{t=T_1}^{T_1+m-1} \{1 - G_Z(z^{ENE}(m) | \theta_t)\} = 1 \quad (11)$$

Meanwhile, if the lifespan of the structure is equal to  $m$ , according to the ADLL method defined by Eqs. (9) and (10), the design value  $z_{T_1-(T_1+m-1)}^{ADLL}(m)$  corresponding to non-exceedance probability  $1 - 1/m$  over the period  $T_1 - (T_1 + m - 1)$  can be calculated as

$$H_{T_1-(T_1+m-1)}(z) = \frac{1}{m} \sum_{t=T_1}^{T_1+m-1} G_Z(z_{T_1-(T_1+m-1)}^{ADLL}(m) | \theta_t) = 1 - 1/m \quad (12)$$

Rearranging Eqs. (11) and (12), the  $m$ -year return level  $z^{ENE}(m)$  can be expressed as

$$z^{ENE}(m) = z_{T_1-(T_1+m-1)}^{ADLL}(m) = H_{T_1-(T_1+m-1)}^{-1}(1 - 1/m) \quad (13)$$

which indicates that ENE and ADLL yield the same design value corresponding to the return period that is consistent with the lifespan of projects.

In addition, if log-transformation is applied to both sides of Eq. (7), i.e., the ER method proposed by Liang et al. (2016), then we obtain

$$\frac{1}{T_2 - T_1 + 1} \sum_{t=T_1}^{T_2} \ln(G_Z(z_{T_1-T_2}^{ER}(m) | \theta_t)) = \ln(1 - 1/m) \quad (14)$$

which is similar to the expression form of the ADLL method in Eq. (10). Thus, the design values calculated by ER and ADLL should be the same, and the ENE method should yield similar design values to those of ER and ADLL.

Furthermore, we can theoretically compare the three return periods calculated for a given design value using Eqs. (5), (7) and (10), which are denoted by  $m_{DLL}$ ,  $m_{ER}$  and  $m_{ADLL}$ , respectively. By using the first-order Taylor series expansions in Eqs. (5), (7) and (10), we can obtain the following approximate mathematical relations:

$$M_{DLL} \approx \frac{m_{ER}}{T_2 - T_1 + 1} \approx \frac{1}{1 - e^{-(T_2 - T_1 + 1)/m_{ADLL}}} \approx \frac{m_{ADLL}}{T_2 - T_1 + 1} \quad (15)$$

It should be noted that the last approximation additionally requires that  $m_{ADLL}$  is slightly larger than  $T_2 - T_1 + 1$ . Typically, these approximations are quite accurate in flood design problems, and the errors can be accurately estimated using the remainder terms of the Taylor series expansion.

#### 2.2. Nonstationary frequency analysis of annual maximum flood series

Under a changing environment, nonstationary frequency analysis is standard practice to deal with the problem of nonstationarity and to perform statistical inference. Many distributions have been investigated to model flood series under stationary conditions. Malamud and Turcotte (2006) and El Adlouni et al. (2008) reviewed the commonly used distributions in flood frequency analysis and categorized them into four groups: the normal family (e.g., normal, lognormal, lognormal type III), the general extreme value (GEV) family (e.g., GEV, Gumbel, Weibull), the Pearson type III family (e.g., gamma, Pearson type III, log-Pearson type III), and the generalized Pareto distribution. Based on the previous classification, three two-parameter distributions, i.e., two-parameter log-normal (LN2), Weibull (WEI), and gamma (GA), and two three-parameter distributions, i.e., Pearson type III (P-III) and GEV, were selected as alternative distributions in this study (Table 1). Under nonstationary conditions, these alternative stationary distributions are extended to account for nonstationarity of the annual maximum flood series (AMFS) using the time-varying moments method built in the framework of Generalized Additive Models in Location, Scale and Shape (GAMLSS) (Rigby and Stasinopoulos, 2005), which has been a popular practice for nonstationary frequency analysis of hydrologic series (Du et al., 2015; Galatsatou et al., 2016; Jiang et al., 2015b; López and Francés, 2013; Villarini et al., 2010;

**Table 1**

Summary of the two-parameter and three-parameter distributions used to model the flood series in the study.

Distributions	Probability density function (PDF)	Distribution moments	Link functions
Lognormal	$f_Z(z \mu, \sigma) = \frac{1}{\sqrt{2\pi}\sigma} \frac{1}{z} \exp\left[-\frac{(\log(z)-\mu)^2}{2\sigma^2}\right]$ $z > 0, \mu > 0, \sigma > 0$	$E(Z) = \omega^{1/2} e^\mu$ $Var(Z) = \omega(\omega - 1)e^{2\mu}$ $\omega = \exp(\sigma^2)$	$h(\mu) = \mu$ $h(\sigma) = \ln(\sigma)$
Gamma	$f_Z(z \mu, \sigma) = \frac{1}{(\mu\sigma^2)^{1/\sigma^2}} \frac{z^{(1/\sigma^2)-1} e^{-z/(\mu\sigma^2)}}{\Gamma(1/\sigma^2)}$ $z > 0, \mu > 0, \sigma > 0$	$E(Z) = \mu$ $Var(Z) = \mu^2 \sigma^2$	$h(\mu) = \ln(\mu)$ $h(\sigma) = \ln(\sigma)$
Weibull	$f_Z(z \mu, \sigma) = \frac{\sigma z^{\sigma-1}}{\mu^\sigma} \exp\left[-\left(\frac{z}{\mu}\right)^\sigma\right]$ $z > 0, \mu > 0, \sigma > 0$	$E(Z) = \mu \Gamma\left(\frac{1}{\sigma} + 1\right)$ $Var(Z) = \mu^2 \{\Gamma\left(\frac{2}{\sigma} + 1\right) - [\Gamma\left(\frac{1}{\sigma} + 1\right)]^2\}$	$h(\mu) = \ln(\mu)$ $h(\sigma) = \ln(\sigma)$
GEV	$f_Z(z \mu, \sigma, \varepsilon) = \frac{1}{\sigma} [1 + \varepsilon\left(\frac{z-\mu}{\sigma}\right)]^{(-1/\varepsilon)-1} \exp\left\{-[1 + \varepsilon\left(\frac{z-\mu}{\sigma}\right)]^{-1/\varepsilon}\right\}$ $-\infty < \mu < \infty, \sigma > 0, -\infty < \varepsilon < \infty$	$E(Z) = \mu - \frac{\sigma}{\varepsilon} \eta_1$ $Var(Z) = \sigma^2 (\eta_2 - \eta_1^2)/\varepsilon^2$ $\eta_m = \Gamma(1 - m\varepsilon)$	$h(\mu) = \mu$ $h(\sigma) = \ln(\sigma)$ $h(\varepsilon) = \varepsilon$
Pearson-III	$f_Z(z \mu, \sigma, \varepsilon) = \frac{1}{\sigma \mu \varepsilon \Gamma(1/\varepsilon^2)} \left(\frac{z-\mu}{\mu \sigma \varepsilon} + \frac{1}{\varepsilon^2}\right)^{\frac{1}{\varepsilon^2}-1} \exp\left[-\left(\frac{z-\mu}{\mu \sigma \varepsilon} + \frac{1}{\varepsilon^2}\right)\right]$ $\sigma > 0, \varepsilon \neq 0, \frac{z-\mu}{\mu \sigma \varepsilon} + \frac{1}{\varepsilon^2} \geq 0$	$E(Z) = \mu$ $C_v = \sigma$ $C_s = 2\varepsilon$	$h(\mu) = \ln(\mu)$ $h(\sigma) = \ln(\sigma)$ $h(\varepsilon) = \varepsilon$

Xiong et al., 2014; Yan et al., 2017). With the time-varying moments method, the location parameter  $\mu_t$  and scale parameter  $\sigma_t$  can be expressed as a linear (with identity link function) or non-linear function (with logarithm link function) of the relevant covariates  $x_j^t$  ( $j = 1, 2, \dots, n$ ) through the monotonic link functions given by

$$\begin{aligned} h(\mu_t) &= \alpha_0 + \sum_{j=1}^n \alpha_j x_j^t \\ h(\sigma_t) &= \beta_0 + \sum_{j=1}^n \beta_j x_j^t \end{aligned} \quad (16)$$

where  $h(\cdot)$  denotes the link function of each statistical parameter, and  $\boldsymbol{\alpha} = (\alpha_0, \dots, \alpha_n)^T$  and  $\boldsymbol{\beta} = (\beta_0, \dots, \beta_n)^T$  represent the parameters for describing  $\mu_t$  and  $\sigma_t$ , respectively.

In the field of nonstationary hydrologic design considering the design lifespan of projects, several previous studies developed non-stationary distributions with either location or scale parameter changing with only a time covariate (Liang et al., 2016; Read and Vogel, 2015; Rootzén and Katz, 2013; Salas and Obeysekera, 2014) or only meteorological covariates (Du et al., 2015; Condon et al., 2015). Here, we derived nonstationary distribution with statistical parameters changing with both a meteorological covariate, i.e., annual total precipitation (*prec*), and a social-economic variable, i.e., population (*pop*), to strengthen the physical meaning of the nonstationary distributions. In the modeling process, for each basin, different covariate combinations were generated, including the use of only the time covariate, *prec* under RCP2.6 and *pop* (scenario 1), *prec* under RCP4.5 and *pop* (scenario 2) and *prec* under RCP8.5 and *pop* (scenario 3). Therefore, for each basin, a total of 20 variation types of statistical parameters were developed (Fig. 1).

In this study, a series of nonstationary distributions were built considering different alternative distributions, variation types of statistical parameters and covariates. Thus, to determine the optimal fitting quality of a model, the Akaike Information Criterion (Akaike, 1974), i.e.,  $AIC = -2 \ln(\zeta) + 2\rho$ , was employed, where  $\zeta$  is the maximized value of the likelihood estimated for each candidate model, and  $\rho$  is the total number of independently adjusted parameters of the model. In addition to the AIC values, diagnostic plots, i.e., the worm plot (van Buuren and Fredriks, 2001) and the centile curves plot, were also inspected to support the model selection and diagnose the fitting performance of the selected optimal models. The worm plot is a useful diagnostic tool for the analysis of residuals and can also be regarded as the detrended Q-Q plot. The centile curves plot presents different percentiles (e.g., 5th, 25th, 50th, 75th and 95th) to assist the visual inspection of probabilistic coverage below different percentiles.

### 2.3. Projections of future precipitation and population

To calculate the future exceedance probabilities which play a fundamental role in the nonstationary hydrologic design and reliability analysis under changing environment, it is necessary to project future precipitation and population covariates for the established nonstationary distributions.

#### 2.3.1. Projections of future precipitation

In recent years, with the improvement of computational capabilities, it has become the most important and frequently used approach to project future climate change using GCMs (General Circulation Models) outputs (Chen et al., 2012, 2016; Arnell and Gosling, 2013; Guo et al., 2012). It should be noted that despite the improvements of GCMs, major uncertainties remain particularly regarding the estimations and projections of precipitation (Kundzewicz and Stakhiv, 2010; Chen et al., 2013).

In this study, we use the statistical downscaling model (SDSM) proposed by Wilby et al. (2002) to bridge the gap between the coarse resolution of GCMs and finer resolution required in local scale studies, see Wilby et al. (2002) for a full technical basis and application of the SDSM method. In the historical period, we initially used SDSM as a perfect prognosis approach to downscale local-scale precipitation using the NCEP (National Center Environmental Prediction) large-scale atmospheric predictors that contain observed information. Since there was a discrepancy between the NCEP and GCM outputs, before downscaling future precipitation, the Quantile Mapping approach was used to eliminate the bias between the NCEP and GCM predictors. Then, the corrected GCM predictors were used to downscale future local-scale precipitation with the calibrated statistical relationship between the NCEP predictors and observed precipitation in the historical period. In this study, annual total precipitation (*prec*) was used as covariate in the nonstationary hydrologic frequency analysis, thus we were more concerned with the capability of the established SDSM model for downscaling annual total precipitation. For this purpose, the generated daily precipitation was aggregated to yearly values during the validation period, and Relative Error ( $R_e$ ) was used to verify the performance of the constructed SDSM model.  $R_e$  is defined as

$$R_e = \frac{|\sum_{i=1}^{\tau} y_i^{obs} - \sum_{i=1}^{\tau} y_i^{sim}|}{\sum_{i=1}^{\tau} y_i^{obs}} \times 100\% \quad (17)$$

where  $y_i^{obs}$  is the observed annual total precipitation in year  $i$ ,  $i = 1, \dots, \tau$ , and  $y_i^{sim}$  is the simulated annual total precipitation in year  $i$ . The closer the value of  $R_e$  is to 0%, the better is the performance of the model.

Based on the established SDSM model with GCMs large-scale predictors as inputs, future daily precipitation can be projected

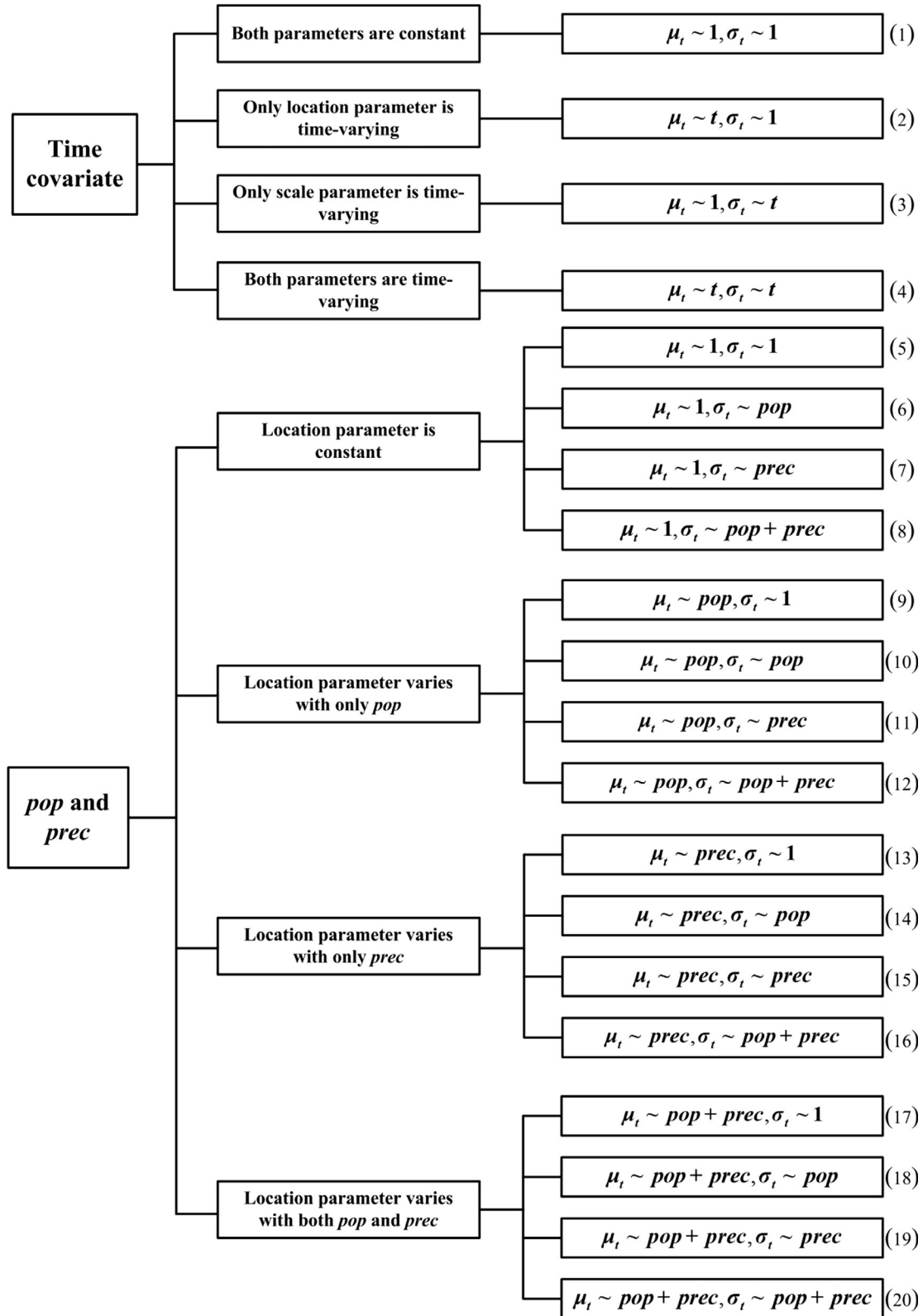


**Fig. 1.** Various variation types for location parameter  $\mu_t$  and scale parameter  $\sigma_t$ . Types (1)–(4) denote variation as functions of only time covariate, while (5)–(20) denote variation as functions of *pop* or *prec* covariates.

and then used to calculate annual total precipitation (*prec*). In this study, 9 different GCMs (BCC, BNU-ESM, CanESM2, CCSM4, CNRM-CM5, GFDL-ESM2M, HadGEM2-ES, MIROC-ESM-CHEM and NorESM1-M) under different emission scenarios (RCP2.6, RCP4.5

and RCP 8.5) were used. To reduce the uncertainty resulting from the variability of outputs from different GCMs, the ensemble mean of 9 GCMs was employed as the covariate, as done by Du et al. (2015). It should be noted that the GCMs outputs are finite with

continuous daily simulations to the year 2100. Although we may fit a model for the estimated GCM outputs and add years beyond 2100 (see the sea level example by Salas and Obeysekera (2014)), apparently, this will add another level of uncertainty for practical application. Thus, by assuming that the hydrologic structures are planned to be in service since 2015, in this study, we only projected future *prec* and associated exceedance probabilities with a maximum timespan of 86 years (i.e., 2100–2015 + 1), which implies: (1) the return periods calculated using the ENE method are limited since the number of return periods is equal to the number of future exceedance probabilities based on Eq. (2); and (2) the design lifespan of hydrologic structures should not exceed the time limit of GCMs outputs. Therefore, in this study, the planning horizon of hydrologic structures was set to 50 years from 2015 to 2064.

### 2.3.2. Projections of future population

Numerous population growth models have been proposed in the literature to model the future growth of the population (Swishchuk and Wu, 2003; Tsoularis and Wallace, 2002; Verhulst, 1838). The simple exponential growth model is able to provide an approximate growth curve for the preliminary period. However, it does not take limited resources and competition into consideration, leading to the continuous growth of the population. Given limited natural resources, unrestricted growth for a population is unrealistic. Therefore, Verhulst (1838) introduced a logistic growth equation to describe the growth of the population by extending the exponential model to incorporate the environmental carrying capacity, which is given by

$$\begin{cases} \frac{dS}{dt} = rS(1 - \frac{S}{S_{max}}) \\ S(t_0) = S_0 \end{cases} \quad (18)$$

where  $r$  is a constant number representing the intrinsic growth rate, and  $S$  denotes the population number.  $S_0$  is the population number at initial time  $t_0$ , and  $S_{max}$  is the maximum population related to the environmental carrying capacity. The Verhulst logistic growth equation has the solution

$$S(t) = \frac{S_{max}}{1 + \left(\frac{S_{max}}{S_0} - 1\right) \exp(-rt)} \quad (19)$$

In this study, the model parameters were estimated using the least squares method. The Verhulst logistic growth equation accommodating growth restriction due to limited natural resources and economic development has been widely used to model population growth. There have been several extensions on the basis of the Verhulst logistic growth model by changing the functional forms of growth but retaining the sigmoidal and asymptotic property of the Verhulst logistic model, see Tsoularis and Wallace (2002) for details.

### 2.4. Estimating confidence intervals using the nonstationary bootstrap method

Quantifying uncertainty of design floods has been an important procedure in conventional statistical inference techniques for hydrologic design under stationary conditions. When considering nonstationary conditions, significant uncertainties arise in the estimation of design floods because the needed distributions are more complex (e.g., additional parameters for modeling the trends of covariates) and the uncertainties associated with future projections provided by various climate models, GCMs, logistic growth models and other techniques. Therefore, to provide a fair comparison among different nonstationary hydrologic design methods, the confidence intervals of design floods were also calculated in this study.

Salas et al. (2013) and Obeysekera and Salas (2014) comprehensively reviewed three different methods, i.e., delta, bootstrap and profile likelihood methods, for generating confidence intervals of design quantiles under stationary and nonstationary conditions, respectively. Based on this, Serinaldi and Kilsby (2015) recommended the use of the bootstrap method because it strictly depends on the available data without any hypotheses and can be easily implemented despite the model complexity. Thus, the nonparametric bootstrap method was used in this study.

The bootstrap method, proposed by Efron (1979), has been widely used by many researchers to quantify uncertainties (Cannon, 2010; Kharin and Zwiers, 2005; Obeysekera and Salas, 2014; Serinaldi and Kilsby, 2015). This section aims to provide a description of the nonstationary nonparametric bootstrap method following Obeysekera and Salas (2014). In the nonstationary case, the original sample observations should be transformed to samples of identically distributed residuals using fitted model parameters before resampling because of the absence of identical distributional assumption for original observations (Cannon, 2010; Coles, 2001; Khalil et al., 2006; Kharin and Zwiers, 2005). Then, the resampling is conducted on the transformed residuals. Taking the nonstationary GEV model with time-varying parameters  $\theta_t = (\mu_t, \sigma_t, \varepsilon_t)$  as an example, the observation data are transformed to a standardized variable  $\tilde{z}$  by

$$\tilde{z}_t = \frac{1}{\varepsilon_t} \ln \left[ 1 + \varepsilon_t \left( \frac{z_t - \mu_t}{\sigma_t} \right) \right] \quad (20)$$

where  $z_t (t = 1, \dots, k)$  is the observation of the extreme hydrologic variable at time  $t$ , and  $\varepsilon_t$  is the shape parameter. The variable  $\tilde{z}_t$  is the  $t$ th transformed residual, which follows a standard Gumbel distribution (Coles, 2001). The selection of the standardized variable contains some degree of arbitrariness. For other nonstationary distributions, we should look for different standardized variables within the same distributional family (Coles, 2001).

The detailed and more general procedure of the nonstationary nonparametric bootstrap method is summarized as follows:

- (1) Fit a nonstationary distribution to the observed samples  $\{z_t, t = 1, \dots, k\}$  and calculate the design quantiles using Eqs. (2), (5), (7) and (10).
- (2) Compute the transformed residuals series  $\tilde{z}_t$  using the model parameters estimated in step (1), based on Eq. (20).
- (3) Resample the transformed residuals  $\tilde{z}_t$  with replacement to obtain a new residual sample series  $\{\tilde{z}_t^b, t = 1, \dots, k\}$ .
- (4) Back-transform the bootstrapped residuals  $\tilde{z}_t^b$  to obtain a new sample of the AMFS, i.e.,  $\{z_t^b, t = 1, \dots, k\}$ , by inverting Eq. (20).
- (5) Fit the bootstrapped data  $z_t^b$  using the same nonstationary distribution established in step (1). Estimate parameters and compute design quantiles using Eqs. (2), (5), (7) and (10).
- (6) Repeat steps (3) to (5) for a large number of times (e.g., 1000), and determine the confidence intervals.

## 3. Study area and data

### 3.1. General description of the three study areas

To illustrate the applications and comparisons of different hydrologic design methods, AMFS of two large basins, i.e., the Weihe River basin (WRB) and the Jinghe River basin (JRB), in China and one small urban basin, i.e., the Assunpink Creek basin (ACB) at Trenton, New Jersey, were analyzed. The three basins were selected for the following reasons: (1) these basins are located in high population density areas that meet the challenges and

demands proposed by the concept of “social-hydrology” (Sivapalan et al., 2012; Savenije et al., 2014) and “hydromorphology” (Vogel, 2011; Vogel et al., 2015) to study the impacts of a growing population combined with human interventions on hydrologic processes; (2) long-term (at least 59 years in our case) daily streamflow, meteorological data and population data are available; and (3) these basins are representative because of their different variation trends in AMFS (decreasing and increasing) and underlying surface conditions (large basins with complex terrain and a small highly urbanized basin).

The Weihe River, which is the longest tributary of the Yellow River, originates from the Gansu province and flows through the southern Loess Plateau. The WRB has an approximate drainage area of 134,800 km<sup>2</sup> and lies between the geographical coordinates 33°40'–37°26'N and 103°57'–110°27'E (Fig. 2). The WRB is located in the transition region from semi-humid to semi-arid and is influenced by the typical temperate continental monsoon climate. The mean annual precipitation of this basin is approximately 544 mm over the period 1951–2012, 60% of which falls in the flood season (from June to September) (Huang et al., 2016). Both the precipitation and streamflow of the WRB exhibit strong inter-annual and seasonal variability. The WRB is the homeland of about 30 million people and is one of the most important industrial and agricultural production zones in western China. In addition, it is the major source of water supply for the state key economic development zone: the Guanzhong Plain. Over the past decades, the total water consumption for industrial purpose, agriculture purpose and residential use has significantly increased on account of the growing population and high-speed development of the economy. The WRB population was approximately 15 million in 1960, while the number doubled by 2012, reaching 30 million. Its average economic growth rate was more than 10% over the past decade. Furthermore, numerous reservoirs and soil and water conservation projects have been constructed in the WRB since the 1950s. Consequently, intense human activities have greatly changed the underlying surface landscape and have further influenced the hydrologic processes in the WRB (Xiong et al., 2015a; Yan et al., 2017; Huang et al., 2016; Jiang et al., 2015a; Chang et al., 2015). It has been observed that the AMFS of the WRB during the period 1951–2012 exhibited significant decreasing trends (Fig. 3).

The Jinghe River, which is located in the Central Loess Plateau, is the longest tributary of the Weihe River and covers the geographical coordinates of 34°46'–37°24'N and 106°14'–109°06'E, with an approximate drainage area of 45,400 km<sup>2</sup> (Fig. 2). The JRB is located in the semiarid region and is influenced by the typical temperate continental monsoon climate. The mean annual precipitation of the JRB is approximately 508 mm over the period 1954–2012, 80% of which falls between June and October. The AMFS in the JRB have been affected by extensive human activities and climate change during the past decades (Chang et al., 2016; Huang et al., 2016). Total water consumption has increased rapidly due to the increases of the population, industrial and agricultural water needs. The population of the JRB has nearly doubled from 1960 (2.1 million) to 2012 (4.7 million). Furthermore, in order to control soil erosion, soil and water conservation measures have taken place since the 1970s, which resulted in a slight increase in vegetation cover (Chen et al., 2008). As shown in Fig. 3, the AMFS observed at the Zhangjiashan station exhibited a decreasing trend over the period 1954–2012.

The third illustrative example focuses on the AMFS of the Assunpink Creek at Trenton, New Jersey, obtained from the United States Geological Survey (USGS) (ID: 01464000). The ACB (40°11'–40°26'N and 74°35'–74°53'W) is located in a highly urbanized area, with an approximate drainage area of 235 km<sup>2</sup> (Fig. 2). The ACB lies in the transition region from humid subtropical to humid continental climate. The average annual precipitation of the ACB is

about 945 mm, which is evenly distributed throughout the year. According to the flow qualification code provided by the USGS (2015), all or part of the AMFS have been affected by urbanization, agricultural changes, channelization or other changes. The population density of the small urban watershed has doubled from the 1930s to the 1990s (Dow and DeWalle, 2000), with the development of economy and urbanization. Besides, a lot of brownfields projects such as urban parks, greenways, and naturalized wetlands have been constructed in the ACB to restore the creek's natural floodplain funded by the U.S. Environmental Protection Agency brownfields program since the 1990s. As shown in Fig. 3, the AMFS of the ACB exhibited an increasing trend over the period 1948–2013, which have been analyzed and discussed in literature focusing on nonstationary hydrologic design (Obeysekera and Salas, 2014, 2016; Serinaldi and Kilsby, 2015).

### 3.2. Data and covariates

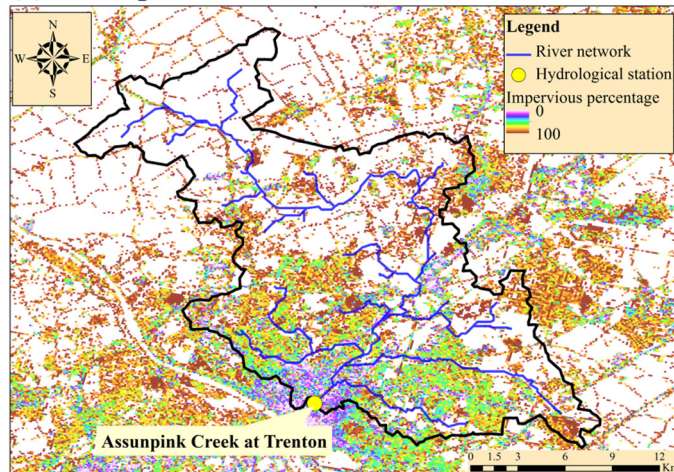
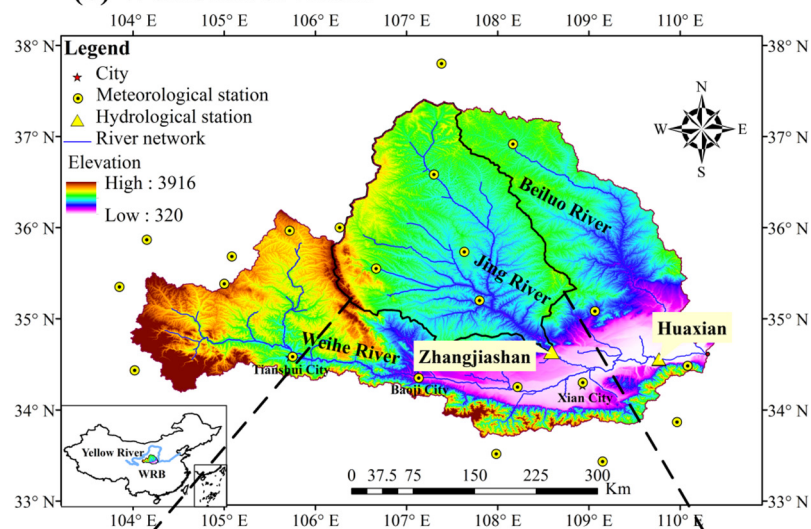
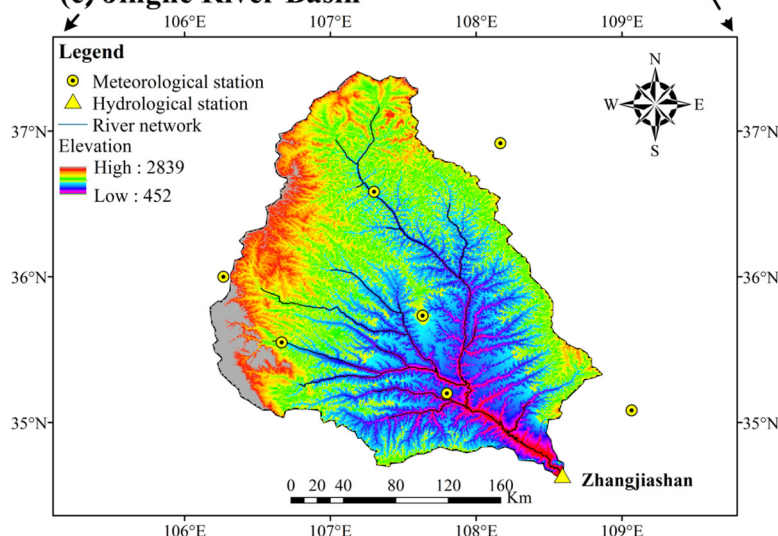
In summary, five categories of data were used in this study, including observed streamflow data, observed meteorological data, population data, NCEP reanalysis data and GCMs outputs from CMIP5.

The observed AMFS of the WRB and JRB for the period 1951–2012 and 1954–2012 were obtained from the Huaxian and Zhangjiashan hydrologic stations, respectively. The Huaxian station is approximately 70 km away from the junction of the Weihe River and Yellow River (Fig. 2b), controlling 80% of the total drainage area of the Weihe River. The Zhangjiashan station is the main gaging station downstream of the Jinghe River, controlling the whole watershed. The observed AMFS of the ACB (1948–2013) were obtained from the USGS gaging station at Trenton (USGS ID: 01464000).

Hydroclimatic and socio-economic covariates, i.e., annual total precipitation (*prec*) and population (*pop*), were used to model the variation of AMFS, since both climatic factors and anthropogenic impacts are considered to have significant effects on streamflow. Precipitation was used to assess the impacts of meteorological factors on the variations of AMFS. Observed daily total precipitation of the 22 meteorological stations located in the WRB was obtained from the National Climate Center of China Meteorological Administration (<http://cdc.cma.gov.cn/>). These data were aggregated to the basin scale using the Thiessen polygon method for the drainage area controlled by the Huaxian and Zhangjiashan stations, respectively. The annual total precipitation series were then calculated according to the created areal mean daily series for the periods 1951–2012 and 1954–2012 for the Huaxian and Zhangjiashan stations, respectively. The historical daily precipitation data of the ACB were derived from the NCEP reanalysis data (source: <http://www.esrl.noaa.gov/>).

As pointed out by Vogel (2011), anthropogenic impacts are prone to interact and manifest themselves in complex ways. Therefore, population, which is a comprehensive index reflecting the mutual effects of urbanization and water consumption, was employed to examine the impacts of the underlying surface landscape on the variations of AMFS, as done by Villarini et al. (2009). The population within each basin was calculated using population data collected by minor civil divisions (e.g., city, township and borough). For the WRB and JRB, annual population data were obtained from the annals of statistics provided by the Shaanxi Provincial Bureau of Statistics (source: <http://www.shaanxitj.gov.cn/>) and Gansu Provincial Bureau of Statistics (source: <http://www.gstj.gov.cn/>). For the ACB, the decennial population data were gathered from the US Census Bureau.

The *pop* and *prec* covariates were standardized by subtracting the mean and dividing by the standard deviation to eliminate the largely different scales of variation between them as done by

**(a) Assunpink Creek Basin****(b) Weihe River Basin****(c) Jinghe River Basin**

**Fig. 2.** (a) Map with the 100-meter resolution impervious area for the Assunpink Creek Basin (ACB), 2013 (Source: [http://nationalmap.gov/small\\_scale/](http://nationalmap.gov/small_scale/)). (b) and (c) are maps of the Weihe River Basin (WRB) and the Jinghe River Basin (JRB), respectively.

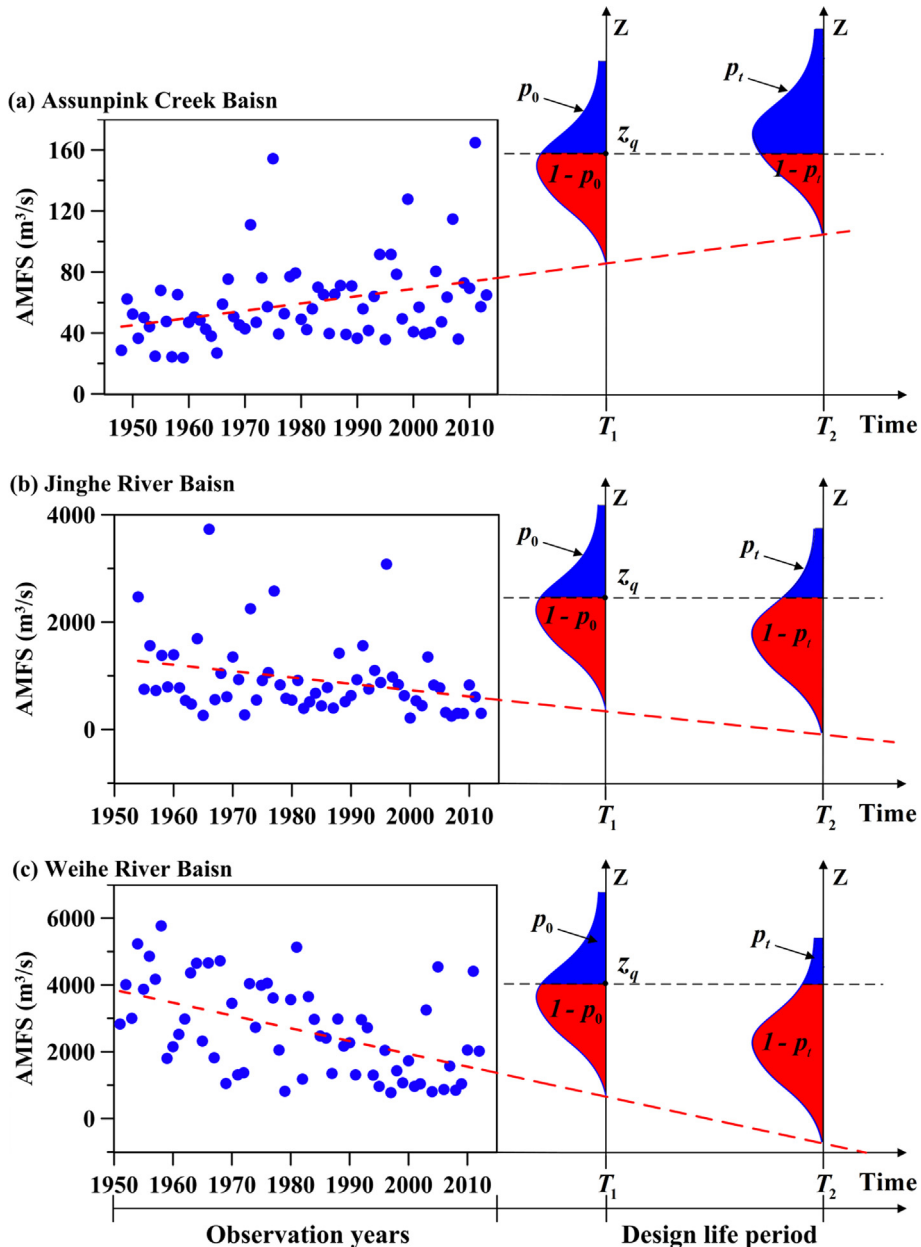


**Fig. 3.** Conceptual sketch for depicting the nonstationarity issue associated with the estimation of design quantiles for a hydrologic structure that assumed to be in service for the period from time  $T_1$  to time  $T_2$ . The red dashed lines represent the different trends of the observations. For the Assunpink Creek Basin (a), there is an increasing exceedance probability  $p_t$  (the blue part of the pdf) with time. For the Jinghe River Basin (b) and Weihe River Basin (c), there are decreasing exceedance probabilities  $p_t$  (the blue part of the pdf) with time. (For interpretation of the references to color in this figure legend, the reader is referred to the web version of this article.)

Villarini and Strong (2014) and Yan et al. (2017). Take the JRB as an illustration, *prec* covariate exhibited a significant variability over the period 1954–2012. While the *pop* covariate exhibited a sigmoidal increasing pattern. A stable period from 1954 to 1960 followed by a rapid increase period 1961–2000, and finally, another stable period 2000–2012 (Fig. 4b).

Two kinds of large-scale atmospheric data, i.e., the NCEP reanalysis daily data and GCMs daily outputs, were employed to establish the statistical downscaling model and generate future scenarios, respectively. The NCEP data were obtained from the NOAA Earth System Research Laboratory (ESRL) (source: <http://www.esrl.noaa.gov/>). The GCMs outputs under three emission scenarios, i.e., RCP2.6 (low emission), RCP4.5 (medium emission) and RCP8.5 (high emission), were available at the CMIP5 website (source: <http://cmip-pcmdi.llnl.gov/cmip5/>). It should be noted

that data pre-processing was conducted since the NCEP and GCMs data were gridded at different spatial scales. Predictors were first interpolated to each meteorological station site using the Inverse Distance Weighting method. Then, areal average series of every predictor for each watershed were calculated using the Thiessen polygon method.

#### 4. Applications and results

##### 4.1. Nonstationary frequency analysis of annual maximum flood series

Preliminary trend detections were first performed for the three AMFS using the Mann-Kendall test (Kendall, 1948; Mann, 1945). Significant increasing trend was detected for the AMFS of Assunpink Creek at 5% significant level with  $p$ -value = 0.012, while sig-

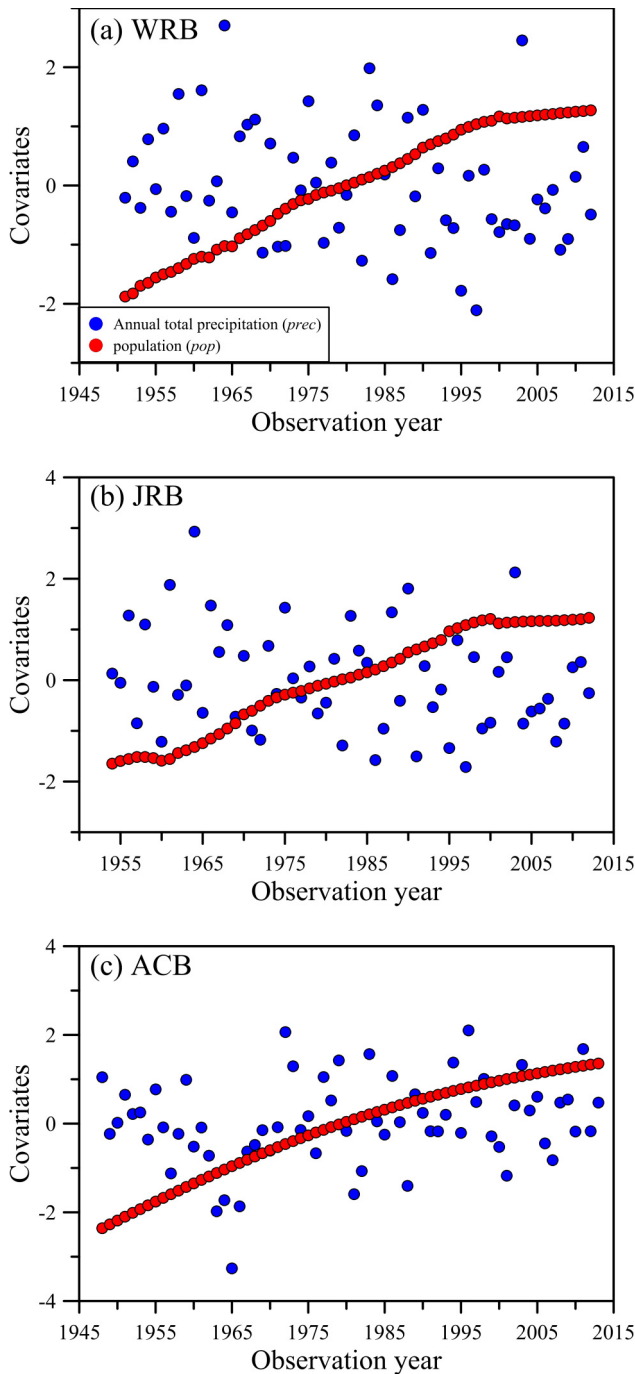


**Fig. 4.** Time series of the two standardized covariates (annual total population and annual total precipitation) of the WRB (a), JRB (b) and ACB (c) used in the modeling of the AMFS. It should be noted that the population of ACB was interpolated based on the estimated logistic growth curve.

nificant decreasing trends were detected for the AMFS of the WRB and JRB at 5% significant level with  $p\text{-value} = 2.12 \times 10^{-5}$  and  $p\text{-value} = 0.012$ , respectively. Then, more robust and detailed frequency analysis of the nonstationary AMFS was implemented under the GAMLS framework.

When modeling the nonstationary AMFS with time covariate, for each basin, a total of 20 models were built considering the different combinations of candidate distributions (5 candidate distributions) and variation types (1 to 4 in Figs. 1 and 5). The model selection procedure was carried out by using the AIC values. For

cases in which different models had very comparable AIC values, model diagnostics were also taken into consideration to provide additional information. The optimal nonstationary models for the three basins are presented in Table 2. To check the goodness-of-fit of the optimal model with time covariate, worm plot and centile curves were employed. For each basin, all scatter points in the worm plot were within the 95% confidence intervals (Fig. 6a–c), indicating good agreement between the selected optimal model and observations. Regarding centile curves, the percentages of observation points below the 5th, 25th, 50th, 75th and 95th centile curves were 3.2%, 33.9%, 45.2%, 69.4% and 95.2% for the WRB; 5.1%, 25.4%, 47.5%, 78.0% and 94.9% for the JRB; and 6.1%, 25.8%, 45.5%, 72.7% and 93.9% for the ACB (Fig. 6d–f), respectively. The above results indicated that the selected models were adequate to model the variability and trend of the observations.

When modeling the nonstationary AMFS with *pop* and *prec*, a total of 80 models were built for each basin, considering the different combinations of candidate distributions (5 candidate distributions) and variation types (5 to 20 in Figs. 1 and 5). Among all possible sub-models, the AIC values suggested that the lognormal distributions with location parameters modeled as a linear function of both *pop* and *prec* were the optimal models for both the WRB and JRB. While for the ACB, the GEV model with a time-varying location parameter and scale parameter was selected as the optimal model (Table 2). The diagnostic results showed that for each basin, all scatter points in the worm plot were within the 95% confidence intervals and aligned smoothly along the blue solid line (Fig. 7a–c), indicating close consistency between the established nonstationary distribution and observations. With respect to the centile curves, the percentages of observation points below the 5th, 25th, 50th, 75th and 95th centile curves were 4.8%, 25.8%, 50.0%, 79.0%, and 93.5% for the WRB; 1.7%, 27.1%, 54.2%, 78.0%, and 93.2% for the JRB; and 7.6%, 28.8%, 40.9%, 80.3% and 92.4% for the ACB, respectively (Fig. 7d–f). The above results indicated that the selected models were adequate to model the variability and trend of the observations.

The above diagnostic results revealed the excellent fitting qualities of the optimal models, either with time covariate or physically-based covariates, in modeling the AMFS of the three basins. In addition, it was also found that for each basin, the optimal model with physically-based covariates had a smaller AIC value than the optimal model with only the time covariate (Table 2), indicating the necessity and superiority of using physically-based covariates as explanatory variables in the nonstationary flood frequency analysis.

#### 4.2. Projections of future precipitation and population

##### 4.2.1. Projections of future precipitation

To examine the capability of the established models for downscaling annual total precipitation (*prec*), Relative Error ( $R_e$ ) between the observed and modeled *prec* were calculated using Eq. (17). It was found that all the established statistical downscaling models performed well for downscaling of *prec*, with  $R_e = 1.2\%$ ,  $R_e = 0.7\%$  and  $R_e = 0.3\%$  for the WRB, the JRB and ACB, respectively.

The future annual total precipitation series of the three basins for the period 2015–2099 were projected based on the constructed downscaling models (Fig. 8). It was found that the 9 GCMs exhibited largely different variation patterns. For the WRB and JRB, the ensemble mean *prec* did not show a significant increasing trend, and the amount of ensemble mean *prec* fluctuated around 500 mm even for higher emission scenarios (RCP4.5 and RCP 8.5). While for the small basin ACB, the increasing trend of the ensemble mean *prec* became more and more significant with the increase of emission scenarios.

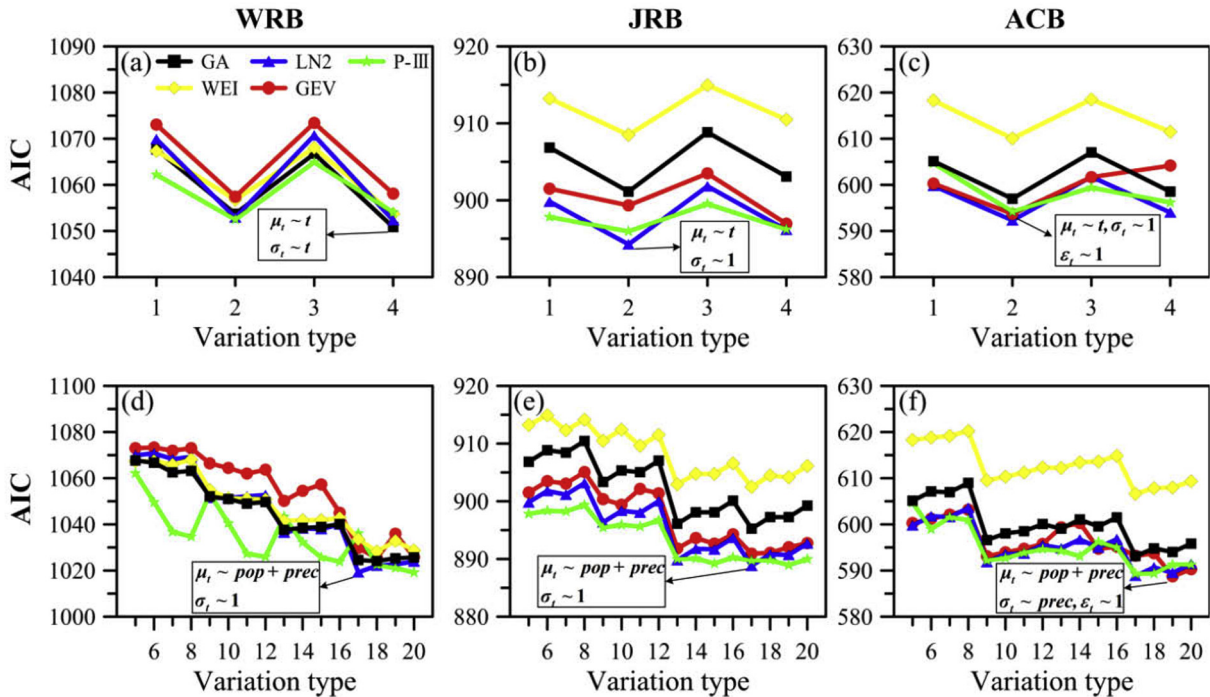


**Fig. 5.** Summary of different nonstationary distributions in modeling the AMFS of WRB, JRB and ACB using time (up panel) as well as using *pop* and *prec* covariates (down panel). The optimal nonstationary distributions are marked by black box. The numbers in the x-axis correspond to each of the 20 variation types defined in Fig. 1, and the values in the y-axis represent their AIC scores.

**Table 2**

Summary of the optimal nonstationary distributions fitted to the AMFS of WRB, JRB and ACB using time and physically-based covariates.  $\alpha_j$  are estimated parameters belonging to location parameter  $\mu_t$ ,  $\beta_j$  are parameters belonging to scale parameter  $\sigma_t$ , and  $\gamma_j$  are parameters belonging to shape parameter  $\varepsilon_t$ . Besides, the significance levels of the estimated parameters are also presented. It should be noted that \*\*\* denotes p value < 0.01; \*\* denotes 0.01 < p value < 0.05; \* denotes 0.05 < p value < 0.1.

Optimal nonstationary distribution		Estimated parameters	AIC
WRB	Nonstationary gamma (time as covariate): $\ln(\mu_t) = \alpha_0 + \alpha_1 \times t$ ; $\ln(\sigma_t) = \beta_0 + \beta_1 \times t$	$\alpha_0 = 8.3110^{***}$ $\alpha_1 = -0.0148^{***}$ $\beta_0 = -1.0748^{***}$ $\beta_1 = 0.0097^*$	1051.84
	Nonstationary lognormal ( <i>pop</i> and <i>prec</i> as covariates): $\mu_t = \alpha_0 + \alpha_1 \times \text{pop} + \alpha_2 \times \text{prec}$ , $\ln(\sigma_t) = \beta_0$	$\alpha_0 = 7.7281^{***}$ $\alpha_1 = -0.2203^{***}$ $\alpha_2 = 0.3230^{***}$ $\beta_0 = -0.9759^{**}$	1021.22
JRB	Nonstationary lognormal (time as covariate): $\mu_t = \alpha_0 + \alpha_1 \times t$ ; $\ln(\sigma_t) = \beta_0$	$\alpha_0 = 7.0144^{***}$ $\alpha_1 = -0.0129^{**}$ $\beta_0 = -0.5176^{**}$	894.26
	Nonstationary lognormal ( <i>pop</i> and <i>prec</i> as covariates): $\mu_t = \alpha_0 + \alpha_1 \times \text{pop} + \alpha_2 \times \text{prec}$ , $\ln(\sigma_t) = \beta_0$	$\alpha_0 = 6.6263^{***}$ $\alpha_1 = -0.1309^*$ $\alpha_2 = 0.2414^{***}$ $\beta_0 = -0.5806^{***}$	888.83
ACB	Nonstationary GEV (time as covariate): $\mu_t = \alpha_0 + \alpha_1 \times t$ ; $\ln(\sigma_t) = \beta_0$ ; $\varepsilon_t = \gamma_0$	$\alpha_0 = 38.1371^{***}$ $\alpha_1 = 0.2701^{**}$ $\beta_0 = 15.6559^{***}$ $\gamma_0 = 0.1905^*$	593.71
	Nonstationary GEV ( <i>pop</i> and <i>prec</i> as covariates): $\mu_t = \alpha_0 + \alpha_1 \times \text{pop} + \alpha_2 \times \text{prec}$ , $\ln(\sigma_t) = \beta_0 + \beta_1 \times \text{prec}$ ; $\varepsilon_t = \gamma_0$	$\alpha_0 = 48.5824^{***}$ $\alpha_1 = 4.3609^{**}$ $\alpha_2 = 4.6781^{***}$ $\beta_0 = 2.6952^{***}$ $\beta_1 = 0.3187^{**}$ $\gamma_0 = 0.1527^*$	588.72

#### 4.2.2. Projections of future population

A total of three logistic growth models were constructed to predict long-term population of the selected basins. As shown in Fig. 9, the observations aligned closely with the fitted growth curve, indicating the good fitting quality of the growth models. All the three growth curves had sigmoidal shapes and were asymptotic to the maximum population until the end of the 21st century. For both the WRB and JRB, there was a sharp increase from the 1950s to 2000s, and then the growth rate declined gradually with the increase of population amount and ultimately reached zero point. While for the ACB, there was a sharp increase from the 1920s to 1970s, after that the population amount gradually reached its carrying capacity.

cating the good fitting quality of the growth models. All the three growth curves had sigmoidal shapes and were asymptotic to the maximum population until the end of the 21st century. For both the WRB and JRB, there was a sharp increase from the 1950s to 2000s, and then the growth rate declined gradually with the increase of population amount and ultimately reached zero point. While for the ACB, there was a sharp increase from the 1920s to 1970s, after that the population amount gradually reached its carrying capacity.

#### 4.3. Comparison results of the four nonstationary hydrologic design methods

Assume that the hydrologic structures of the three basins are planned to be in service from 2015 to 2064, with a lifespan of 50 years. Having obtained the projected future *pop* and *prec* covariates, the selected optimal nonstationary distributions with either time or physically-based covariates (Table 2) were employed to calculate the exceedance probability  $p_t$ , and ultimately used to compute the design floods using the ENE, DLL, ER and ADLL approaches. In addition, their associated bootstrapped 95% confidence intervals were also estimated to provide a fair comparison among the different approaches.

As discussed in the section of methodology, for the same predetermined design value, the corresponding return periods calculated by the three different nonstationary design methods of DLL, ER and ADLL have the approximate relationships expressed by Eq. (15), as the reliability over the whole project life span is considered by DLL in contrast to the average yearly reliability considered by both ER and ADLL. With the consideration of Eq. (15), it should be noted that, in comparing the design values calculated by different nonstationary design methods, for a given value of return period  $m$  defined in terms of the average yearly reliability, the values of  $z_{T_1-T_2}^{ER}(m)$  and  $z_{T_1-T_2}^{ADLL}(m)$  should be compared against

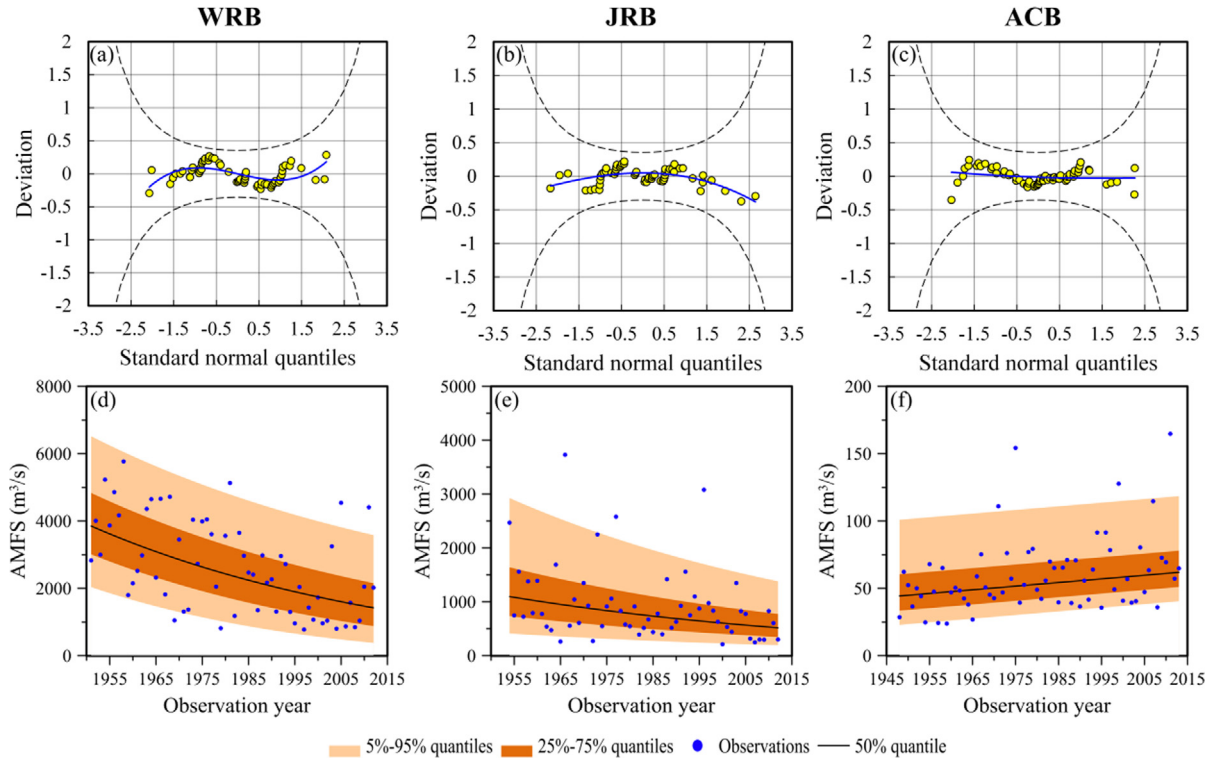


**Fig. 6.** Diagnostic plots for evaluating the goodness-of-fit of the optimal nonstationary distributions using time covariate for the three basins. (a), (b) and (c) are worm plots; (d), (e) and (f) are the centiles curves plots.

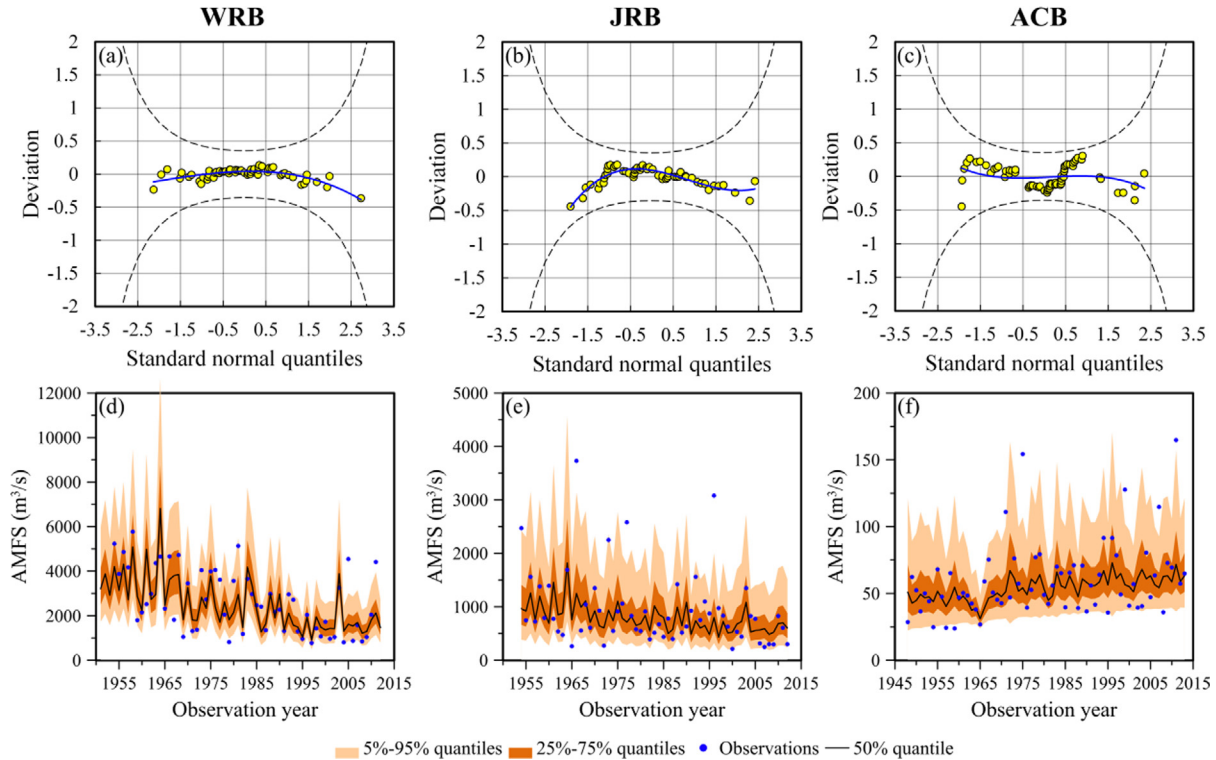


**Fig. 7.** Diagnostic plots for evaluating the goodness-of-fit of the optimal nonstationary distributions using *pop* and *prec* covariates for the three basins. (a), (b) and (c) are worm plots; (d), (e) and (f) are the centiles curves plots.

$z_{T_1-T_2}^{\text{DLL}} \left( \frac{m}{T_2-T_1+1} \right)$  rather than against  $z_{T_1-T_2}^{\text{DLL}}(m)$  to compare design values at the same risk level, when  $m$  is larger than  $T_2 - T_1 + 1$ .

To generate a visualized comparison among different methods, Figs. 10–13 summarized the nonstationary design results calculated by ENE, ER and ADLL for a range of return periods

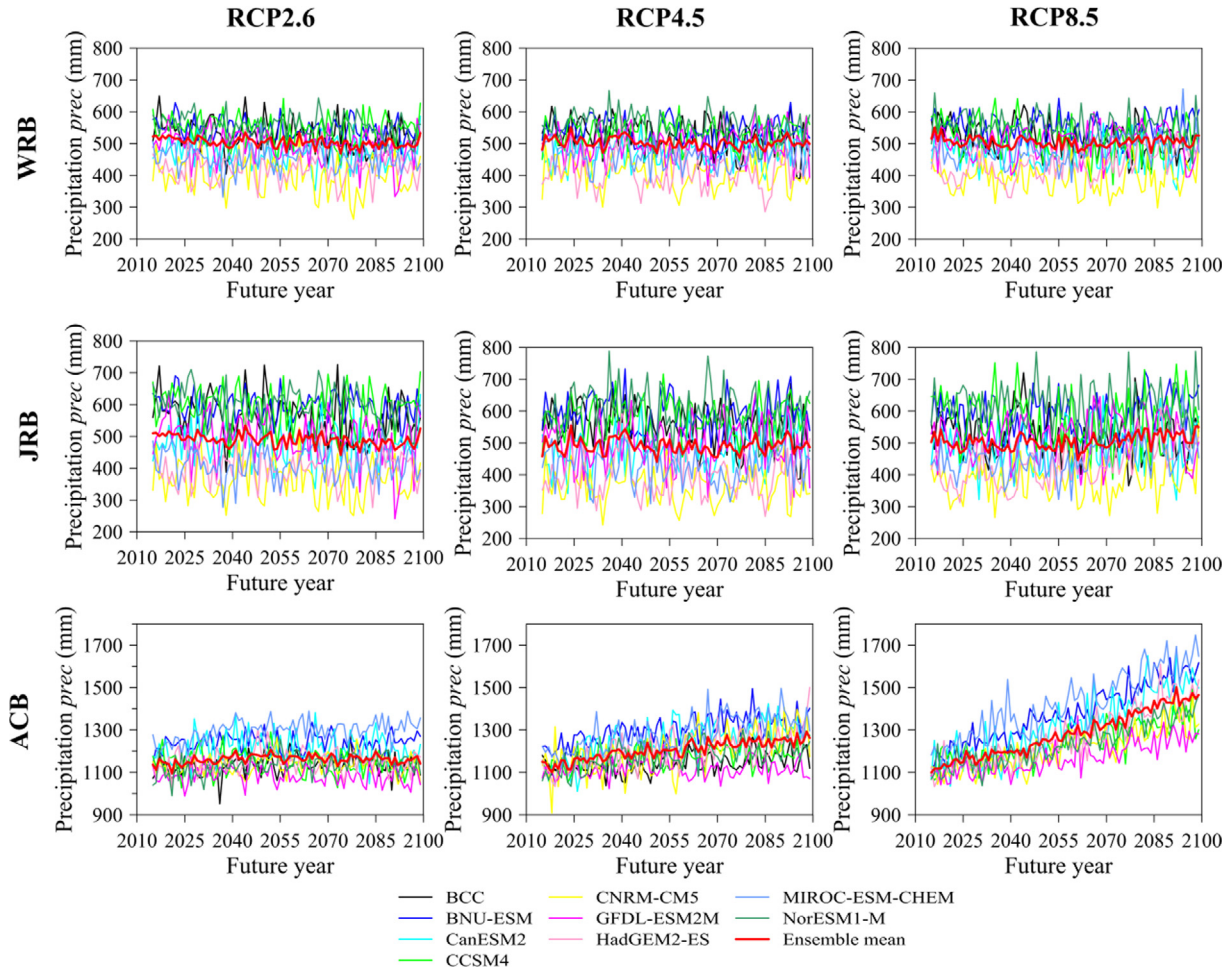


**Fig. 8.** Projected annual total precipitation *prec* by using outputs of different GCMs under three different emission scenarios (RCP2.6, RCP4.5 and RCP 8.5) for the period of 2015–2099. The ensemble mean is the arithmetic mean value of the 9 GCMs.

$m \in [2, 1000]$  under the time covariate scenario and three different physically-based covariate scenarios (*prec* under different RCPs and the same *pop*). Meanwhile, to provide a fair comparison between DLL and other three methods, design values calculated by DLL for  $m_{DLL} \in [2, 20]$ , which corresponds to  $m \in [100, 1000]$  according to Eq. (15), were also plotted in Figs. 10–13. Fig. 10 displayed that, for all three study basins and for return period  $m \in [2, 1000]$ , ENE, ER and ADLL in general yielded the same or very similar design values and confidence intervals when the time covariate scenario was considered. The exception was the ENE method for the AMFS with decreasing trends (the WRB and JRB), in which case the design quantiles based on ENE were smaller than those values of both ER and ADLL and became almost constant for larger return period  $m \in [200, 1000]$  due to that the exceedance probabilities in the far future could decrease to zero. Also, it was found from Fig. 10 that DLL yields similar design values for  $m \in [100, 1000]$  or  $m_{DLL} \in [2, 20]$  if the relationship between DLL and ER/ADLL return periods, i.e. Eq. (15), was taken into account. From Figs. 11–13, the same conclusion can be drawn with respect to the comparison of these four nonstationary design methods under three different physically-based covariate scenarios (*prec* under different RCPs and the same *pop*).

Moreover, it was also found that the design values calculated by ER and ADLL were nearly overlapped with each other for a range of  $m \in [2, 1000]$ , which is in consistence with the approximate mathematical relations between ER and ADLL based on Eqs. (14) and (15). In addition, ENE and ADLL yielded the same design value

for the return period  $m = 50$ , which is equal to the assumed planning horizon of projects in this paper, and similar design quantiles and confidence intervals for the other return periods. This is expected since ENE is a special case of ADLL when the return period is equal to the planning horizon of projects based on Eqs. (11)–(13).

Besides, in terms of the covariate, for the WRB, the design quantiles calculated using the time covariate were larger than those using physically-based covariates and had obviously wider confidence intervals. For the JRB and ACB, however, the design quantiles calculated using the time covariate were lower than those using the physically-based covariates and contained comparative or smaller confidence intervals. These results highlight the difference caused by the use of different nonstationary distributions and covariates. It should be noted that we also calculated design values using the GEV distribution for the WRB and JRB and found similarities between the GEV results and lognormal results.

## 5. Conclusions and discussions

Nonstationary hydrologic design under a changing environment is one of the most important issues and research focuses in hydrology. This paper aims to highlight the significance of considering a project's design life period in nonstationary hydrologic design. For this purpose, we compared the four nonstationary design methods, namely the ENE, DLL, ER and ADLL methods, using the

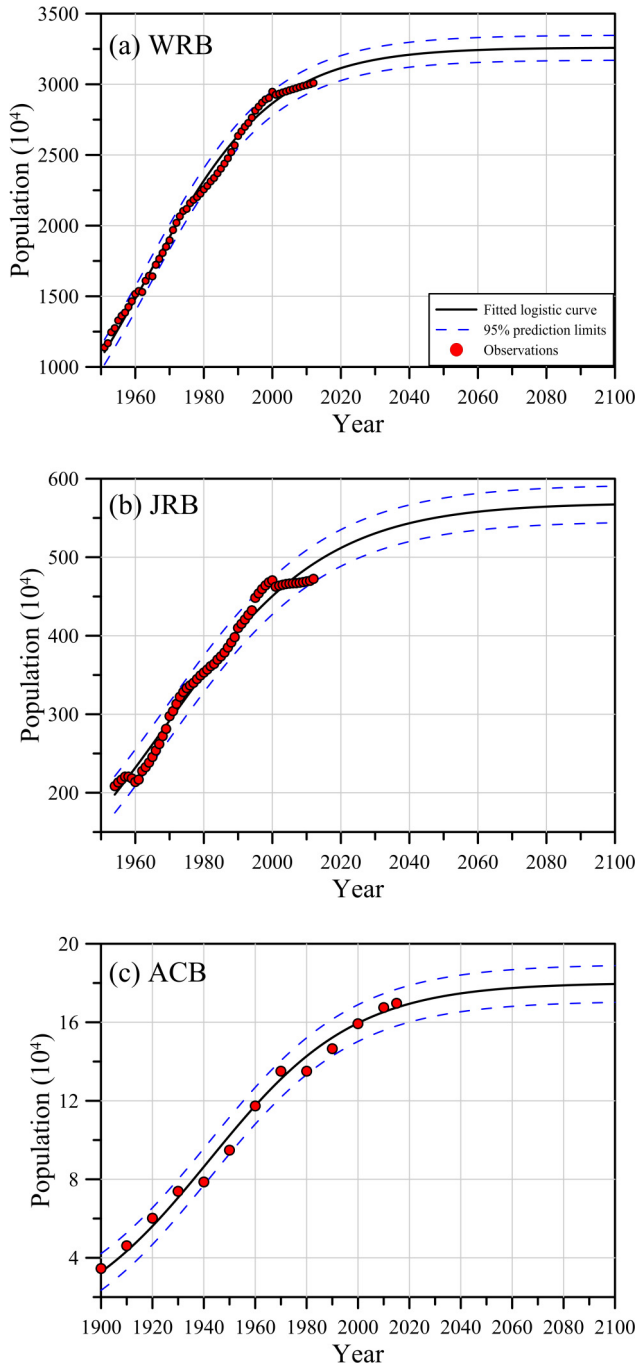


**Fig. 9.** Logistic population growth curves of (a) the WRB for the period of 1951–2099, (b) the JRB for the period of 1954–2099, (c) the ACB for the period of 1900–2099. The red solid circles are the observations. The black solid lines are the fitted logistic curves and the blue dashed lines are the upper and lower 95% prediction limits. It should be noted decennial population data was provided by the US Census Bureau.

AMFS of the Weihe River basin, Jinghe River basin, and Assunpink Creek basin as illustrations. The main conclusions of this study are as follows:

- (1) The AMFS of the WRB, the JRB and ACB have exhibited significant decreasing or increasing trend due to climate change and human activities. For the WRB, the nonstationary lognormal model with the location parameter  $\mu_t$  modeled as a function of both  $pop$  and  $prec$  was the optimal model. For

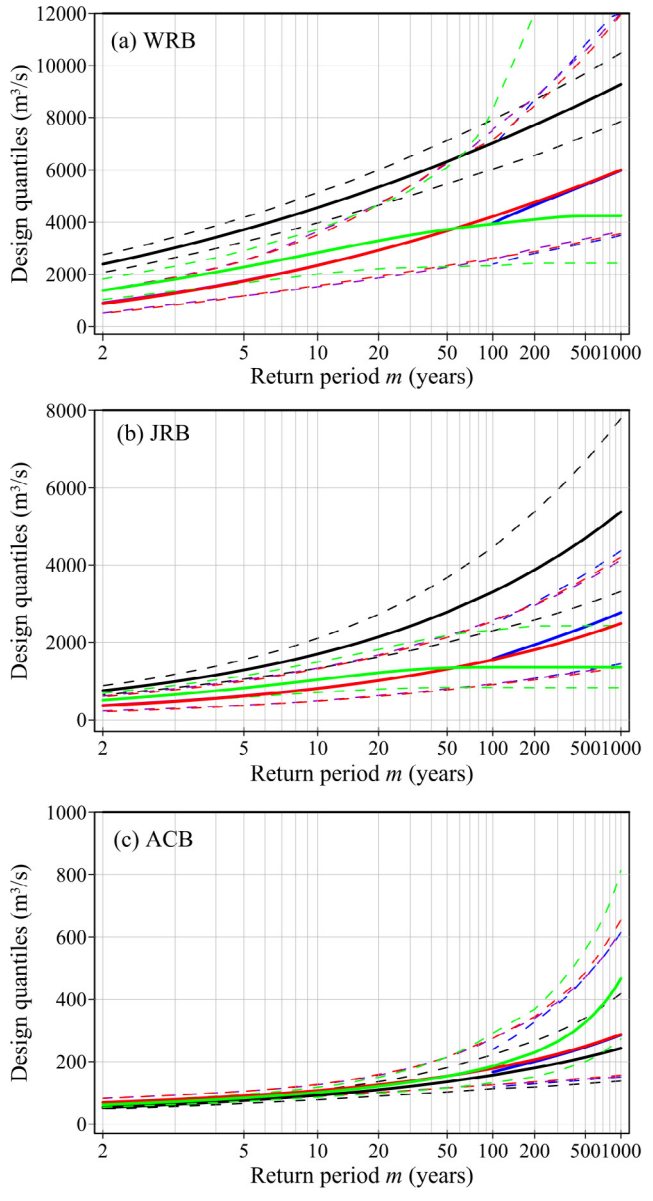
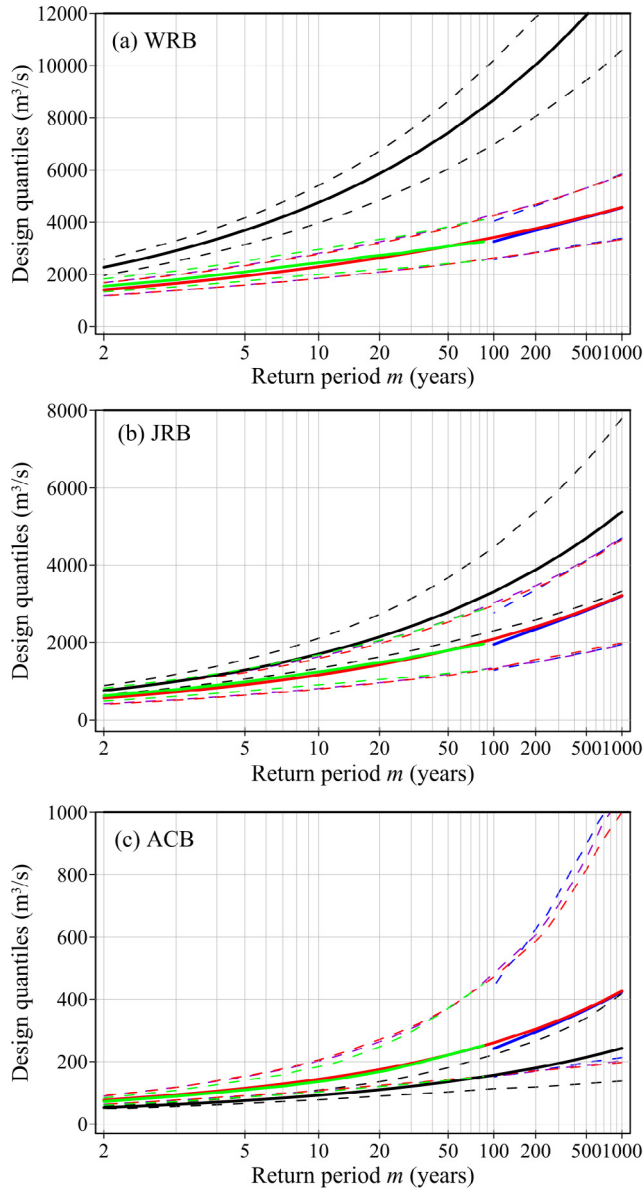


**Fig. 10.** Return level diagrams for (a) WRB, (b) JRB and (c) ACB resulting from different design approaches (ENE, DLL, ER and ADLL) using the time covariate with 95% bootstrapped confidence intervals.

the JRB, the nonstationary lognormal model with the time-varying location parameter was the optimal model. The location parameter  $\mu_t$  was expressed as a function of both  $pop$  and  $prec$ . For the ACB, the nonstationary GEV model with both time-varying location and scale parameters was the optimal model, whose  $\mu_t$  was expressed as a function of both  $pop$  and  $prec$ , and the log-transformed  $\sigma_t$  was expressed as a function of only  $prec$ . Additionally, we also found that among all the optimal models, the two-parameter lognormal distribution was an excellent and parsimonious model for representing the distribution of AMFS, which is consistent with the recommendation of other researchers (Prosdocimi et al., 2014; Read and Vogel, 2015; Stedinger and Crainiceanu, 2000; Villarini et al., 2009; Vogel et al., 2011).



Stationary reference: — Design floods — — Upper and lower limit of 95% CIs  
 ENE: — Design floods — — Upper and lower limit of 95% CIs  
 DLL: — Design floods — — Upper and lower limit of 95% CIs  
 ER: — Design floods — — Upper and lower limit of 95% CIs  
 ADLL: — Design floods — — Upper and lower limit of 95% CIs

**Fig. 11.** Return level diagrams for WRB (a), JRB (b) and ACB (c) using different design approaches (ENE, DLL, ER and ADLL) with 95% bootstrapped confidence intervals under the covariate scenario 1. The covariate scenario 1 refers to the projected *prec* under RCP2.6 and *pop*. The solid lines are the design floods while the dashed lines are the upper and lower limits of the 95% confidence intervals.

- (2) It was also found that for all the study basins, when performing nonstationary flood frequency analysis, the overall performance of the optimal nonstationary distributions using the socio-economic covariate (*pop*) and meteorological covariate (*prec*) was better than those using only the time covariate as explanatory variable according to the AIC scores and diagnostic plots, indicating the stronger explanatory power of the socio-economic and climatic variables for the nonstationary flood frequency analysis.
- (3) The nonstationary design quantiles and associated confidence intervals calculated by ENE, ER and ADLL were very similar, since ENE or ER was a special case or had a similar

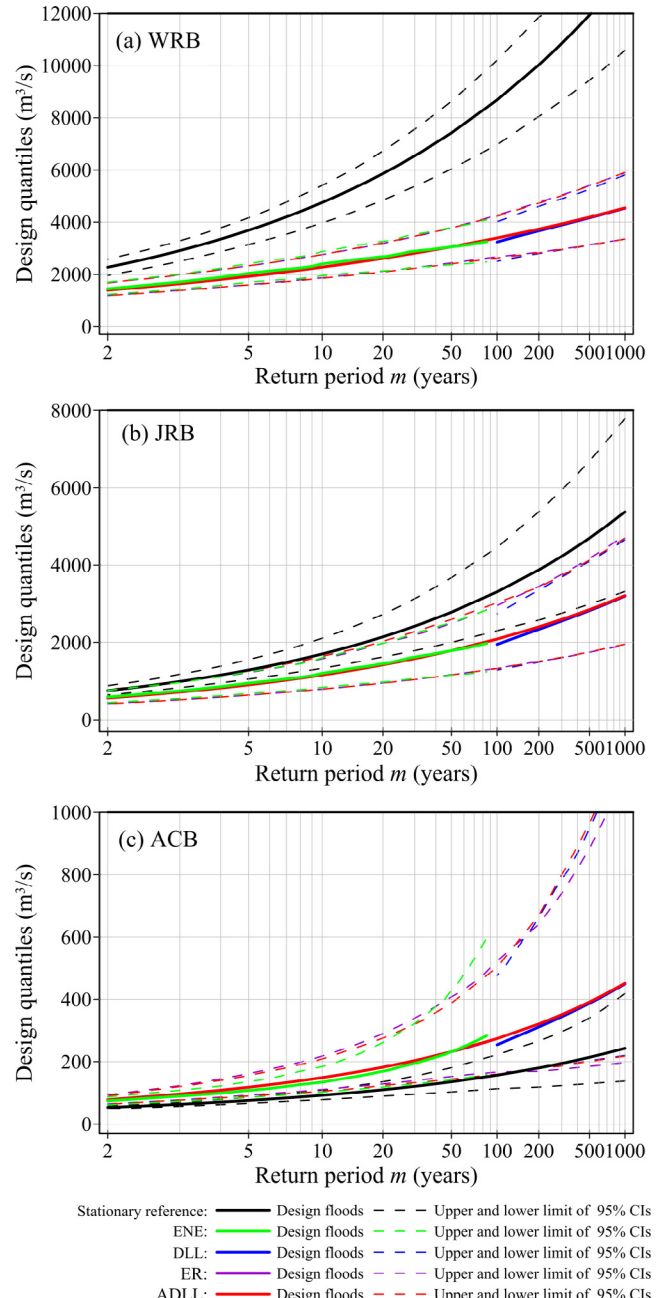


**Fig. 12.** Return level diagrams for WRB (a), JRB (b) and ACB (c) using different design approaches (ENE, DLL, ER and ADLL) with 95% bootstrapped confidence intervals under the covariate scenario 2. The covariate scenario 2 refers to the projected *prec* under RCP4.5 and *pop*. The solid lines are the design floods while the dashed lines are the upper and lower limits of the 95% confidence intervals.

expression form with respect to ADLL. In particular, the design quantiles calculated by ENE and ADLL were the same when return period was equal to the length of the design life. In addition, DLL yields similar design values if the relationship between DLL and ER/ADLL return periods, i.e. Eq. (15), is considered. Furthermore, ENE, ER and ADLL had good adaptability to either an increasing or decreasing situation, yielding not too large or too small design quantiles. This is important for applications of nonstationary hydrologic design methods in actual practice because of the concern of choosing the emerging nonstationary methods versus the traditional stationary based methods. There is still a long

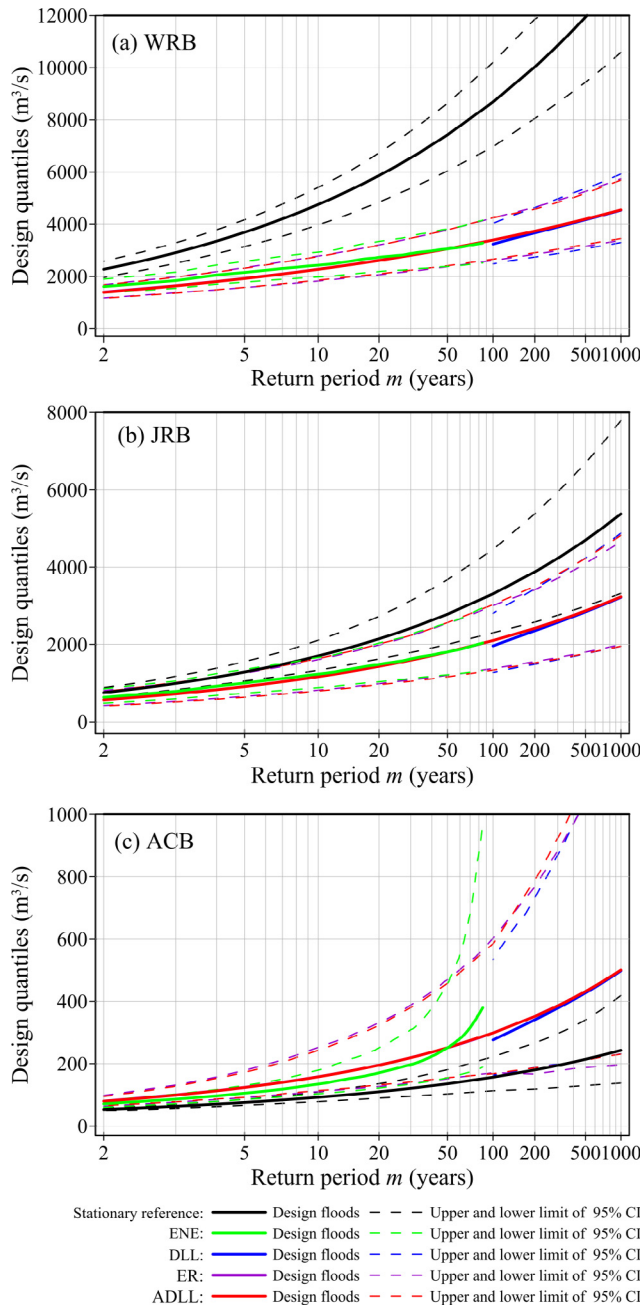


**Fig. 13.** Return level diagrams for WRB (a), JRB (b) and ACB (c) using different design approaches (ENE, DLL, ER and ADLL) with 95% bootstrapped confidence intervals under the covariate scenario 3. The covariate scenario 3 refers to the projected *prec* under RCP8.5 and *pop*. The solid lines are the design floods while the dashed lines are the upper and lower limits of the 95% confidence intervals.

way to go for the conceptual transition from stationarity to nonstationarity. Although ENE yielded similar design quantiles and confidence intervals with other methods, it did not account for the design life of the project, and its applications were restricted to the associated timespan of the projected covariates, e.g., if we want to estimate a design quantile corresponding to  $m = 100$  or  $1000$ , we must obtain projected covariates extending to the future 100 or 1000 years, which will definitely bring about higher levels of uncertainties. ER and ADLL aimed to address the nonstationary hydrologic design issue in terms of reliability. These two approaches depicted the joint time-varying distribu-

tions within the design life period of the projects, needing no additional information of exceedance probabilities beyond the project's design lifespan. Furthermore, ER enabled us to solve the design problems under nonstationarity by adopting the stationary design reliability, thus bridging the gap between stationary and nonstationary design criteria.

Following the above three major conclusions, several comments on the applications of nonstationary hydrologic design methods are also made as follows:

First, one should be very cautious when performing nonstationary frequency analysis under a changing environment. As reported by many studies, the hydrologic system has been altered by substantial climate change and human activities. Under the famous assertion of "stationarity is dead" made by Milly et al. (2008), nearly every conventional and fundamental method in hydrologic science needs to be accommodated to account for increased nonstationarity (Vogel, 2011). Nonstationary hydrologic frequency analysis theory emerges at the moment in response to this concern, aiming to improve the understanding and interpretation of changing properties of hydrologic systems. However, as discussed by Milly et al. (2015), the exploration of appropriate approaches for addressing the nonstationarity issue presented by climate change and human activities remains a challenge. Clearly, the nonstationary hydrologic frequency analysis theory is far from perfect and has recently been questioned by a series of thoughtful and well-founded papers (Koutsoyiannis and Montanari, 2014; Lins and Cohn, 2011; Montanari and Koutsoyiannis, 2014; Serinaldi and Kilsby, 2015). The academic debate focuses on the definition and interpretation of the scientific concept of stationarity and the reliability of the nonstationary distributions to make future predictions considering the significant uncertainties involved in the more complicated model structure of nonstationary distributions and the uncertainties of future projections. Indeed, change does not automatically imply nonstationarity and stationarity does not imply at all unchanging process state (Montanari and Koutsoyiannis, 2014; Xiong et al., 2015b). Therefore, nonstationarity cannot be determined only from the view of statistical tests of finite or usually short observations but should be comprehensively confirmed via attribution analysis, statistical analysis, or empirical analysis.

Second, nonstationary hydrologic design theory needs to be carefully tested and correctly applied in the real-world. In this respect, this paper evaluates the performance of nonstationary hydrologic frequency analysis and presents a fair comparison among different nonstationary hydrologic design methods. However, to reduce the uncertainties involved in the nonstationary distributions in this study, the model structures of nonstationary distributions were set to be relatively simple with a linear trend in the distribution parameters, which could be unrealistic. Furthermore, under the framework of the time-varying moments method, the physical meaning of the estimated model parameters  $\alpha = (\alpha_0, \dots, \alpha_n)^T$  for  $\mu_t$  and (or)  $\beta = (\beta_0, \dots, \beta_n)^T$  for  $\sigma_t$  are ambiguous, for lack of clear physical meanings. Therefore, new model structures that can better describe the changing properties of flood events and strengthen the physical meaning of estimated parameters  $\alpha$  and  $\beta$  should be pursued in future studies.

Third, in nonstationary hydrologic design, the modeling of the future evolution of the distribution, which relies heavily on the projections of explanatory variables or covariates, is also one of the most challenging issues (Obeysekera and Salas, 2016; Serinaldi and Kilsby, 2015). The covariates selected for nonstationary modeling should satisfy two requirements: (1) having sufficient explanatory power to describe the changing properties of

flood frequency; and (2) being able to provide reliable predictions. In this study, *pop* and *prec* were chosen as covariates because that they are closely related to the changing flood process due to climatic factors and human intervention, and can be predicted using relatively mature population growth models and climate models. In particular, *pop* is regarded as a reflection of the intensity of human activities and can serve as a simple characterization of urbanization or land use. However, it has limitations in depicting the physical processes related to flood frequency, compared with direct analysis using predictions of future land use changes (Obeysekera and Salas, 2016; Serinaldi and Kilsby, 2015; Villarini et al., 2009). Thus, it is necessary to explore more explanatory variables that have stronger physical associations with the process of flood events, as well as improve the reliability of future projections in future studies.

Finally, the stationary assumption and its associated frequency analysis method are conservative but reliable planning strategies, which could still play an important role in practical engineering, regardless of whether our world is stationary or not. By contrast, nonstationary hydrologic design is aimed at what should be done when nonstationarity is really true, thus providing alternative approaches for decision-makers. Regarding nonstationary hydrologic design, one of the goals of this study was to push forward the practical applications of nonstationary design methods. Thus, in this study, the four methods were unified into a general framework through a transformation formula  $m = 1/(1 - RRE)$  between representative reliability (*RRE*) and the return period. It should be noted that this transformation may limit the flexibility of risk based methods to some extent. It should also be mentioned that the approaches presented in this paper provide a general framework for flood design under nonstationarity and can be extended for applications under the POT context, as has been successfully realized by the ENE approach in other studies (Parey et al., 2010; Obeysekera and Salas, 2016). Besides, new approaches that can improve the understanding of climatic and anthropogenic impacts on the hydrologic system and manage or balance the uncertainties of the nonstationary modeling, e.g., by combining physically-based hydrologic models and statistical models, should be pursued.

## Acknowledgments

This research is financially supported by the National Natural Science Foundation of China (Grants 51525902, 51190094 and 51479139), which are greatly appreciated. Great thanks are due to the editor and three reviewers, as their comments are all valuable and very helpful for improving the quality of this paper.

## References

- Akaike, H., 1974. A new look at the statistical model identification. *IEEE T. Automat. Contr.* 19 (6), 716–723.
- Arnell, N.W., Gosling, S.N., 2013. The impacts of climate change on river flow regimes at the global scale. *J. Hydrol.* 486, 351–364.
- Buchanan, M.K., Kopp, R.E., Oppenheimer, M., Tebaldi, C., 2016. Allowances for evolving coastal flood risk under uncertain local. *Climatic Change* 137 (3), 347–362.
- Cannon, A.J., 2010. A flexible nonlinear modelling framework for nonstationary generalized extreme value analysis in hydroclimatology. *Hydrol. Process.* 24 (6), 673–685.
- Chang, J., Wang, Y., Istanbulluoglu, E., Bai, T., Huang, Q., Yang, D., Huang, S., 2015. Impact of climate change and human activities on runoff in the Weihe River basin. *China. Quatern. Int.* 380–381, 169–179.
- Chang, J., Zhang, H., Wang, Y., Zhu, Y., 2016. Assessing the impact of climate variability and human activities on streamflow variation. *Hydrol. Earth Syst. Sci.* 20 (4), 1547–1560.
- Chen, C., Xie, G., Zhen, L., Leng, Y., 2008. Analysis on Jinghe watershed vegetation dynamics and evaluation on its relation with precipitation. *Acta Ecologica Sinica* 28 (3), 925–938.
- Chen, H., Xu, C.-Y., Guo, S., 2012. Comparison and evaluation of multiple GCMs, statistical downscaling and hydrological models in the study of climate change impacts on runoff. *J. Hydrol.* 434–435, 36–45.
- Chen, J., Brisette, F.P., Lucas-Picher, P., 2016. Transferability of optimally-selected climate models in the quantification of climate change impacts on hydrology. *Clim. Dyn.* 47, 3359–3372.
- Chen, J., Brisette, F.P., Chaumont, D., Braun, M., 2013. Finding appropriate bias correction methods in downscaling precipitation for hydrologic impact studies over North America. *Water Resour. Res.* 49, 4187–4205.
- Coles, S., 2001. An Introduction to Statistical Modeling of Extreme Values. Springer, London, England.
- Condon, L.E., Gangopadhyay, S., Pruitt, T., 2015. Climate change and non-stationary flood risk for the upper Truckee River basin. *Hydrol. Earth Syst. Sci.* 19 (1), 159–175.
- Cooley, D., 2013. Return periods and return levels under climate change. In: AghaKouchak, A., Easterling, D., Hsu, K., Schubert, S., Sorooshian, S. (Eds.), *Extremes in a Changing Climate*. Springer, Dordrecht, Netherlands, pp. 97–114.
- Dow, C.L., DeWalle, D.R., 2000. Trends in evaporation and Bowen Ratio on urbanizing watersheds in eastern United States. *Water Resour. Res.* 36 (7), 1835–1843.
- Du, T., Xiong, L., Xu, C.-Y., Gippel, C.J., Guo, S., Liu, P., 2015. Return period and risk analysis of nonstationary low-flow series under climate change. *J. Hydrol.* 527, 234–250.
- Efron, B., 1979. Bootstrap methods: another look at the jackknife. *Ann. Stat.* 7 (1), 1–26.
- El Adlouni, S., Bobée, B., Ouarda, T.B.M.J., 2008. On the tails of extreme event distributions in hydrology. *J. Hydrol.* 355 (1–4), 16–33.
- Galiatsatou, P., Agnastopoulou, C., Prinos, P., 2016. Modeling nonstationary extreme wave heights in present and future climates of Greek Seas. *Water Sci. Eng.* 9 (1), 21–32.
- Gilroy, K.L., McCuen, R.H., 2012. A nonstationary flood frequency analysis method to adjust for future climate change and urbanization. *J. Hydrol.* 414, 40–48.
- Guo, J., Chen, H., Xu, C.-Y., Guo, S., Guo, J., 2012. Prediction of variability of precipitation in the Yangtze River basin under the climate change conditions based on automated statistical downscaling. *Stoch. Env. Res. Risk A.* 26 (2), 157–176.
- Huang, S., Liu, D., Huang, Q., Chen, Y., 2016. Contributions of climate variability and human activities to the variation of runoff in the Weihe River basin. *China. Hydrol. Sci. J.* 61 (6), 1026–1039.
- Jiang, C., Xiong, L., Wang, D., Liu, P., Guo, S., Xu, C.-Y., 2015a. Separating the impacts of climate change and human activities on runoff using the Budyko-type equations with time-varying parameters. *J. Hydrol.* 522, 326–338.
- Jiang, C., Xiong, L., Xu, C.-Y., Guo, S., 2015b. Bivariate frequency analysis of nonstationary low-flow series based on the time-varying copula. *Hydrol. Process.* 29 (6), 1521–1534.
- Katz, R.W., Parlange, M.B., Naveau, P., 2002. Statistics of extremes in hydrology. *Adv. Water Resour.* 25 (8), 1287–1304.
- Kendall, M.G., 1948. Rank Correlation Methods. Griffin, Oxford, England.
- Khaliq, M.N., Ouarda, T.B.M.J., Ondo, J.C., Gachon, P., Bobée, B., 2006. Frequency analysis of a sequence of dependent and/or non-stationary hydro-meteorological observations: a review. *J. Hydrol.* 329 (3–4), 534–552.
- Kharin, V.V., Zwiers, F.W., 2005. Estimating extremes in transient climate change simulations. *J. Climate* 18 (8), 1156–1173.
- Koutsoyiannis, D., Montanari, A., 2014. Negligent killing of scientific concepts: the stationarity case. *Hydrol. Sci. J.* 60 (7–8), 1174–1183.
- Kundzewicz, Z.W., Stakhiv, E.Z., 2010. Are climate models “ready for prime time” in water resources management applications, or is more research needed? *Editorial. Hydrol. Sci. J.* 55 (7), 1085–1089.
- Liang, Z., Hu, Y., Huang, H., Wang, J., Li, B., 2016. Study on the estimation of design value under non-stationary environment. *South-to-North Water Transfers Water Sci. Technol.* 14 (1), 50–53 (in Chinese with English abstract).
- Lins, H.F., Cohn, T.A., 2011. Stationarity: wanted dead or alive? *J. Am. Water Resour. Assoc.* 47 (3), 475–480.
- López, J., Francés, F., 2013. Non-stationary flood frequency analysis in continental Spanish rivers, using climate and reservoir indices as external covariates. *Hydrol. Earth Syst. Sci. Discuss.* 17 (8), 3103–3142.
- Malamud, B.D., Turcotte, D.L., 2006. The applicability of power-law frequency statistics to floods. *J. Hydrol.* 322 (1–4), 168–180.
- Mann, H.B., 1945. Nonparametric tests against trend. *Econometrica* 13 (3), 245–259.
- Milly, P.C.D., Betancourt, J., Falkenmark, M., Hirsch, R., Kundzewicz, Z.W., Lettenmaier, D.P., Stouffer, R.J., Dettinger, M.D., Krysanova, V., 2015. On critiques of “Stationarity is Dead: Whither Water Management?”. *Water Resour. Res.* 51 (9), 7785–7789.
- Milly, P.C.D., Betancourt, J., Falkenmark, M., Hirsch, R.M., Kundzewicz, Z.W., Lettenmaier, D.P., Stouffer, R.J., 2008. Stationarity is dead: whither water management? *Science* 319 (5863), 573–574.
- Mondal, A., Mujumdar, P.P., 2015. Return levels of hydrologic droughts under climate change. *Adv. Water Resour.* 75, 67–79.
- Montanari, A., Young, G., Savenije, H.H.G., Hughes, D., Wagener, T., Ren, L.L., Koutsoyiannis, D., Cudennec, C., Toth, E., Grimaldi, S., 2013. “Panta Rei—Everything Flows”: change in hydrology and society-The IAHS Scientific Decade 2013–2022. *Hydrol. Sci. J.* 58 (6), 1256–1275.
- Montanari, A., Koutsoyiannis, D., 2014. Modeling and mitigating natural hazards: stationarity is immortal! *Water Resour. Res.* 50 (12), 9748–9756.
- Obeysekera, J., Salas, J., 2014. Quantifying the uncertainty of design floods under nonstationary conditions. *J. Hydrol. Eng.* 19 (7), 1438–1446.
- Obeysekera, J., Salas, J., 2016. Frequency of recurrent extremes under nonstationarity. *J. Hydrol. Eng.* 21 (5), 04016005.

- Olsen, R., Lambert, J.H., Haimes, Y.Y., 1998. Risk of extreme events under nonstationary conditions. *Risk Anal.* 18, 497–510.
- Parey, S., Hoang, T.T.H., Dacunha Castelle, D., 2010. Different ways to compute temperature return levels in the climate change context. *Environmetrics* 21 (7–8), 698–718.
- Parey, S., Malek, F., Laurent, C., Dacunha-Castelle, D., 2007. Trends and climate evolution: statistical approach for very high temperatures in France. *Climatic Change* 81 (3–4), 331–352.
- Prosdocimi, I., Kjeldsen, T.R., Svensson, C., 2014. Non-stationarity in annual and seasonal series of peak flow and precipitation in the UK. *Nat. Hazards Earth Syst. Sci.* 14 (5), 1125–1144.
- Read, L.K., Vogel, R.M., 2015. Reliability, return periods, and risk under nonstationarity. *Water Resour. Res.* 51 (8), 6381–6398.
- Read, L.K., Vogel, R.M., 2016. Hazard function analysis for flood planning under nonstationarity. *Water Resour. Res.* 52 (5), 4116–4131.
- Rigby, R.A., Stasinopoulos, D.M., 2005. Generalized additive models for location, scale and shape. *J. Roy. Stat. Soc. C – Appl. Stat.* 54 (3), 507–554.
- Rootzén, H., Katz, R.W., 2013. Design life level: quantifying risk in a changing climate. *Water Resour. Res.* 49 (9), 5964–5972.
- Salas, J., Heo, J., Lee, D., Burlando, P., 2013. Quantifying the uncertainty of return period and risk in hydrologic design. *J. Hydrol. Eng.* 18 (5), 518–526.
- Salas, J.D., Obeysekera, J., 2014. Revisiting the concepts of return period and risk for nonstationary hydrologic extreme events. *J. Hydrol. Eng.* 19 (3), 554–568.
- Savenije, H.H.G., Hoekstra, A.Y., van der Zaag, P., 2014. Evolving water science in the anthropocene. *Hydrol. Earth Syst. Sci.* 18 (1), 319–332.
- Serinaldi, F., 2015. Dismissing return periods! *Stoch. Environ. Res. Risk A* 29 (4), 1179–1189.
- Serinaldi, F., Kilby, C.G., 2015. Stationarity is undead: uncertainty dominates the distribution of extremes. *Adv. Water Resour.* 77, 17–36.
- Sivapalan, M., Savenije, H.H.G., Blöschl, G., 2012. Socio-hydrology: a new science of people and water. *Hydrol. Process.* 26 (8), 1270–1276.
- Stedinger, J.R., Crainiceanu, C.M., 2000. Climate variability and flood-risk management. *Risk-Based Decision Making in Water Resources*, vol. 9. American Society of Civil Engineers, Reston, pp. 77–86.
- Swishchuk, A., Wu, J., 2003. Logistic Growth Models. *Mathematical Modelling: Theory and Applications*, vol. 18. Springer, Dordrecht, Netherlands, pp. 175–185.
- Tsoularis, A., Wallace, J., 2002. Analysis of logistic growth models. *Math. Biosci.* 179 (1), 21–55.
- USGS, 2015. Surface water for the USA: peak streamflow. U.S. Department of the Interior, USGS, Washington, DC. (<http://nwis.waterdata.usgs.gov/usa/nwis/peak>) (May, 2015).
- van Buuren, S., Fredriks, M., 2001. Worm plot: a simple diagnostic device for modelling growth reference curves. *Stat. Med.* 20 (8), 1259–1277.
- Verhulst, P., 1838. Notice sur la loi que la population suit dans son accroissement. *Correspondance Mathématique et Physique Publiée par A Quetelet* 10, 113–121.
- Villarini, G., Smith, J.A., Serinaldi, F., Bales, J., Bates, P.D., Krajewski, W.F., 2009. Flood frequency analysis for nonstationary annual peak records in an urban drainage basin. *Adv. Water Resour.* 32 (8), 1255–1266.
- Villarini, G., Scoccimarro, E., White, K.D., Arnold, J.R., Schilling, K.E., Ghosh, J., 2015. Projected changes in discharge in an agricultural watershed in Iowa. *J. Am. Water Resour. Assoc.* 51 (5), 1361–1371.
- Villarini, G., Strong, A., 2014. Roles of climate and agricultural practices in discharge changes in an agricultural watershed in Iowa. *Agric. Ecosyst. Environ.* 188, 204–211.
- Villarini, G., Smith, J.A., Napolitano, F., 2010. Nonstationary modeling of a long record of rainfall and temperature over Rome. *Adv. Water Resour.* 33 (10), 1256–1267.
- Vogel, R., 2011. *Hydromorphology*. *J. Water Res. Plan. Man.* 137 (2), 147–149.
- Vogel, R.M., Lall, U., Cai, X., Rajagopalan, B., Weiskel, P.K., Hooper, R.P., Matalas, N.C., 2015. Hydrology: the interdisciplinary science of water. *Water Resour. Res.* 51 (6), 4409–4430.
- Vogel, R.M., Yaindl, C., Walter, M., 2011. Nonstationarity: flood magnification and recurrence reduction factors in the United States1. *J. Am. Water Resour. Assoc.* 47 (3), 464–474.
- Wilby, R.L., Dawson, C.W., Barrow, E.M., 2002. SDSM – a decision support tool for the assessment of regional climate change impacts. *Environ. Modell. Software* 17 (2), 145–157.
- Xiong, L., Du, T., Xu, C.-Y., Guo, S., Jiang, C., Gippel, C.J., 2015a. Non-Stationary annual maximum flood frequency analysis using the norming constants method to consider non-stationarity in the annual daily flow series. *Water Resour. Manag.* 29 (10), 3615–3633.
- Xiong, L., Jiang, C., Xu, C.-Y., Yu, K., Guo, S., 2015b. A framework of change-point detection for multivariate hydrological series. *Water Resour. Res.* 51 (10), 8198–8217.
- Xiong, L., Jiang, C., Du, T., 2014. Statistical attribution analysis of the nonstationarity of the annual runoff series of the Weihe River. *Water Sci. Technol.* 70 (5), 939–946.
- Yan, L., Xiong, L., Liu, D., Hu, T., Xu, C.-Y., 2017. Frequency analysis of nonstationary annual maximum flood series using the time-varying two-component mixture distributions. *Hydrol. Process.* 31 (1), 69–89.